The Making and Breaking of the Himalayan Arc

Malay Mukul

malaymukul@iitb.ac.in

http://www.geos.iitb.ac.in/index.php/mm

HIMALAYAN ARC

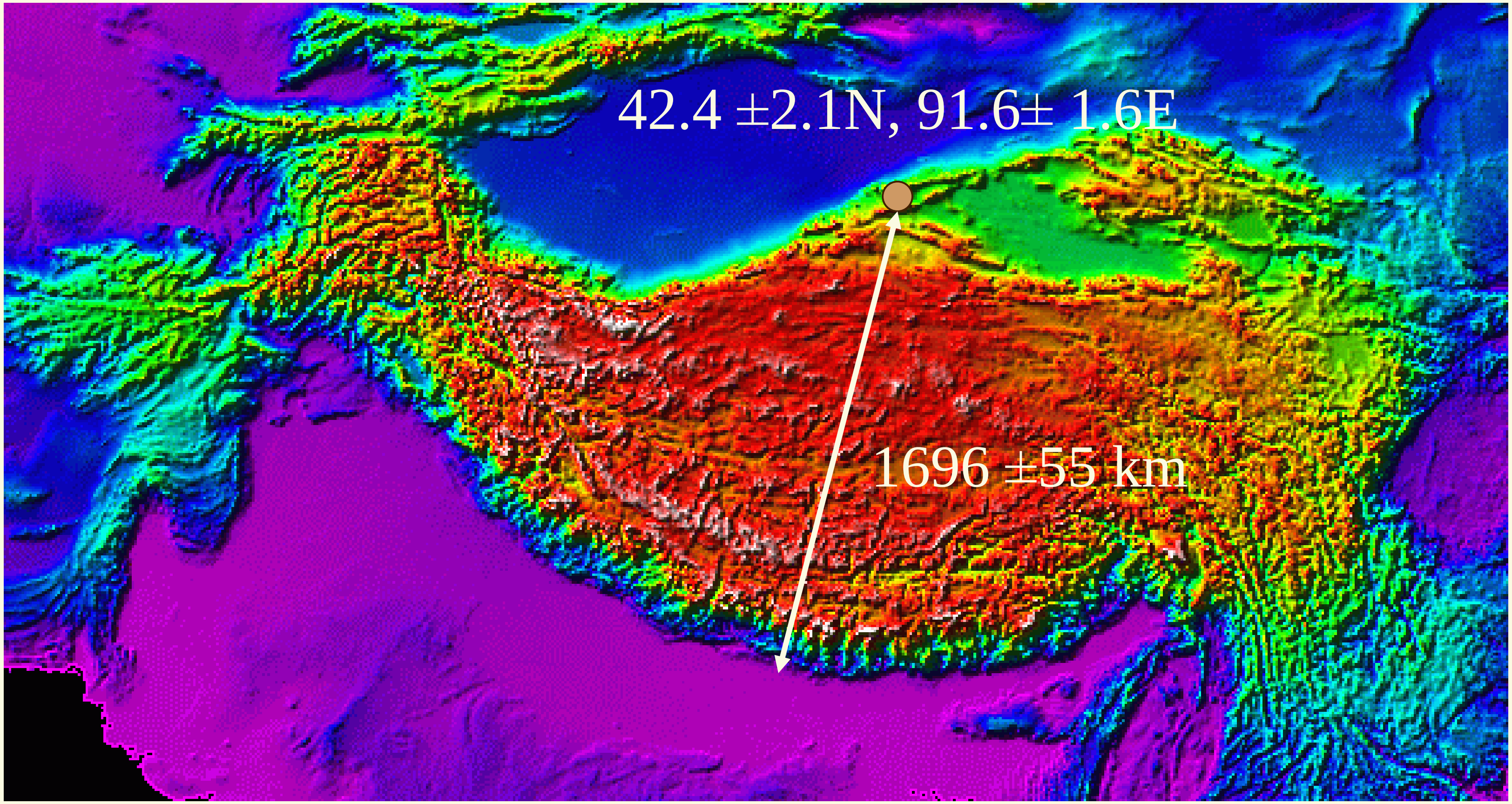

http://www.geo.cornell.edu/grads/duncan/topo/topo.gif

(Bendick and Bilham, Geology, 2001)

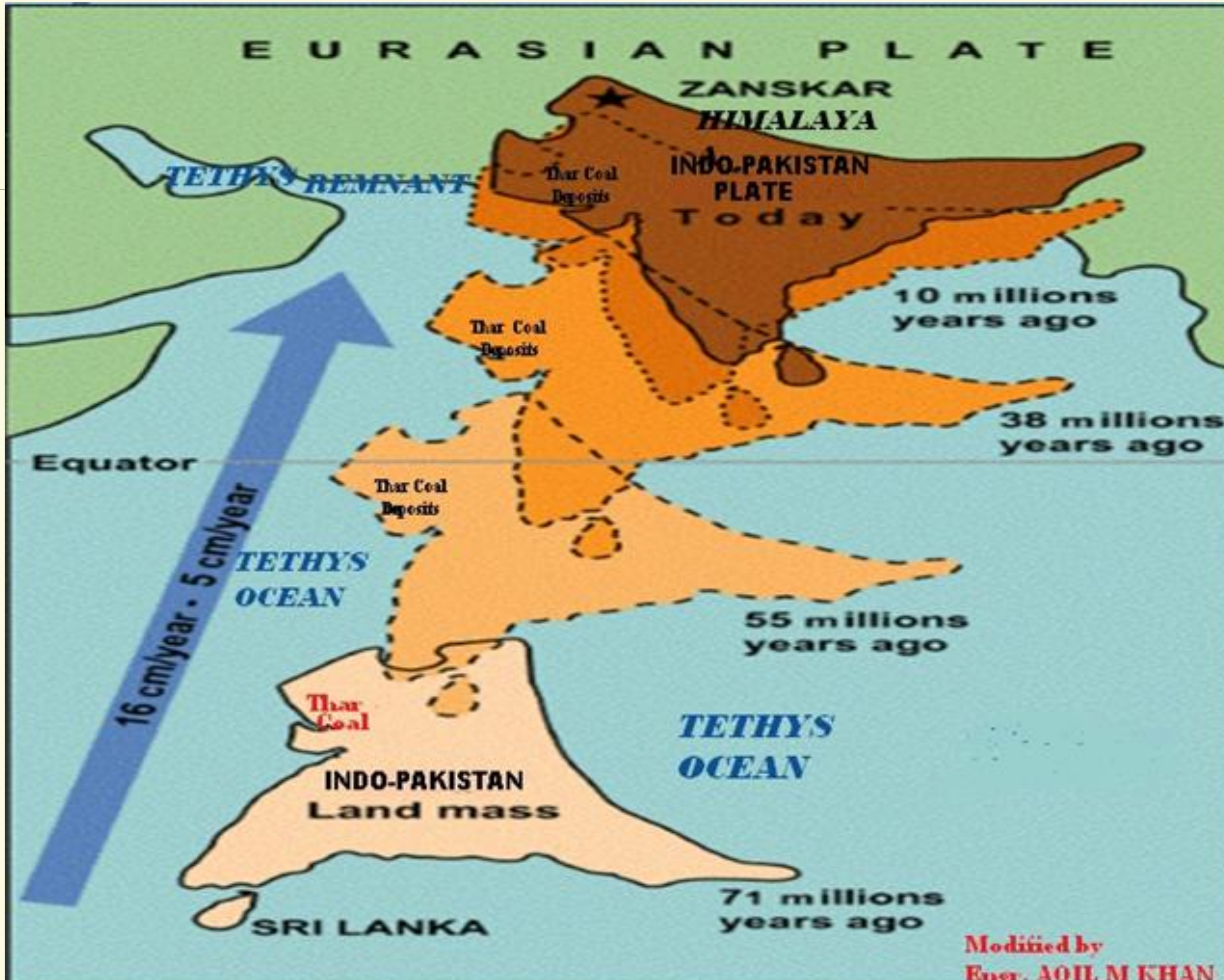

EURASIAN PLATE
ZANSKAR
HIMALAYA
INDO-PAKISTAN
PLATE
Today
TETHYS REMNANT
Thar Coal
Deposits
10 millions
years ago
Thar Coal
Deposits
38 millions
years ago
Equator
Thar Coal
Deposits
16 cm/year - 5 cm/year
TETHYS
OCEAN
55 millions
years ago
Thar
Coal
TETHYS
OCEAN
INDO-PAKISTAN
Land mass
71 millions
years ago
SRI LANKA
Modified by
Engr. AQIL M KHAN

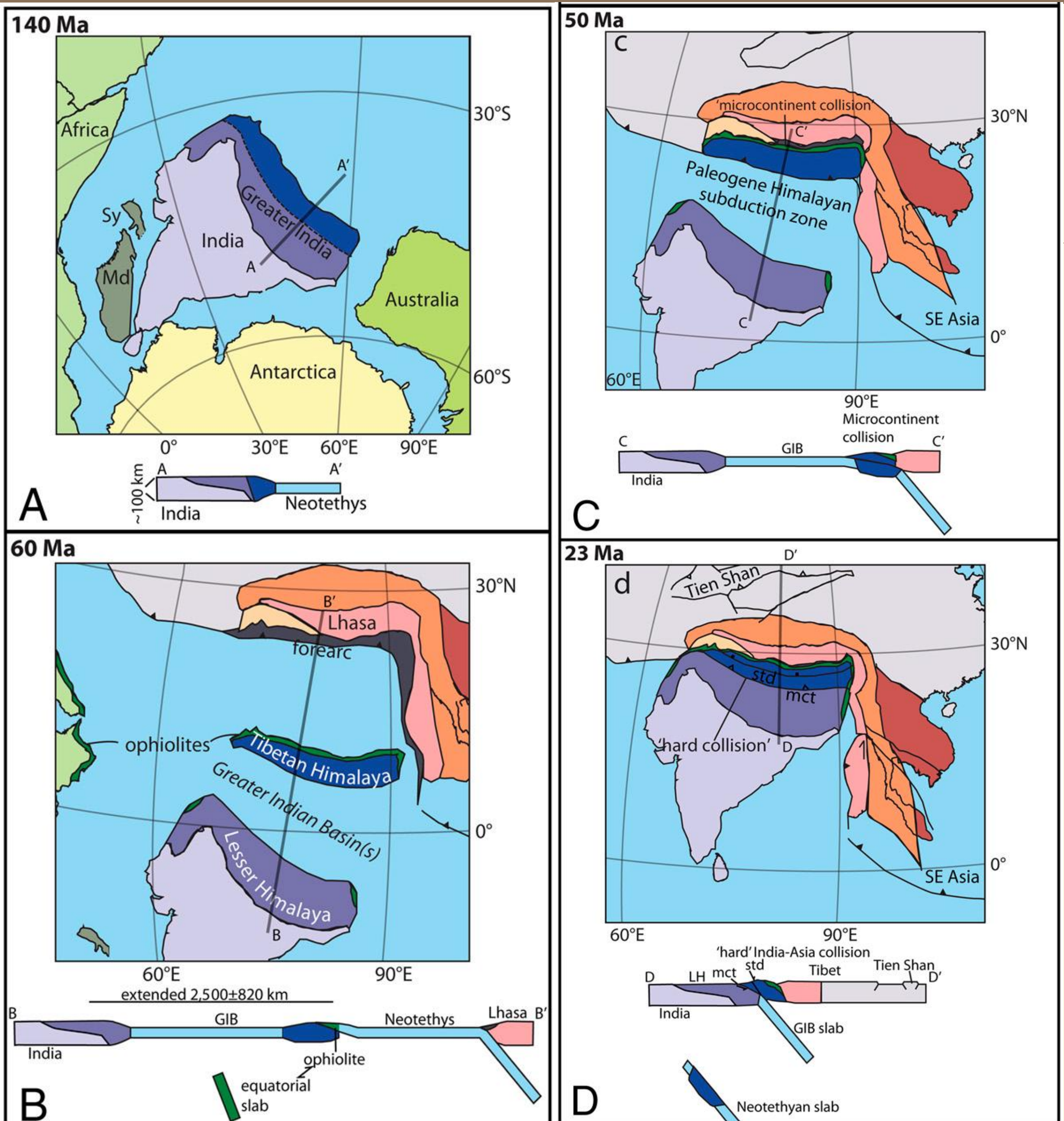

van Hinsbergen et al., 2012

MAKING THE ARC

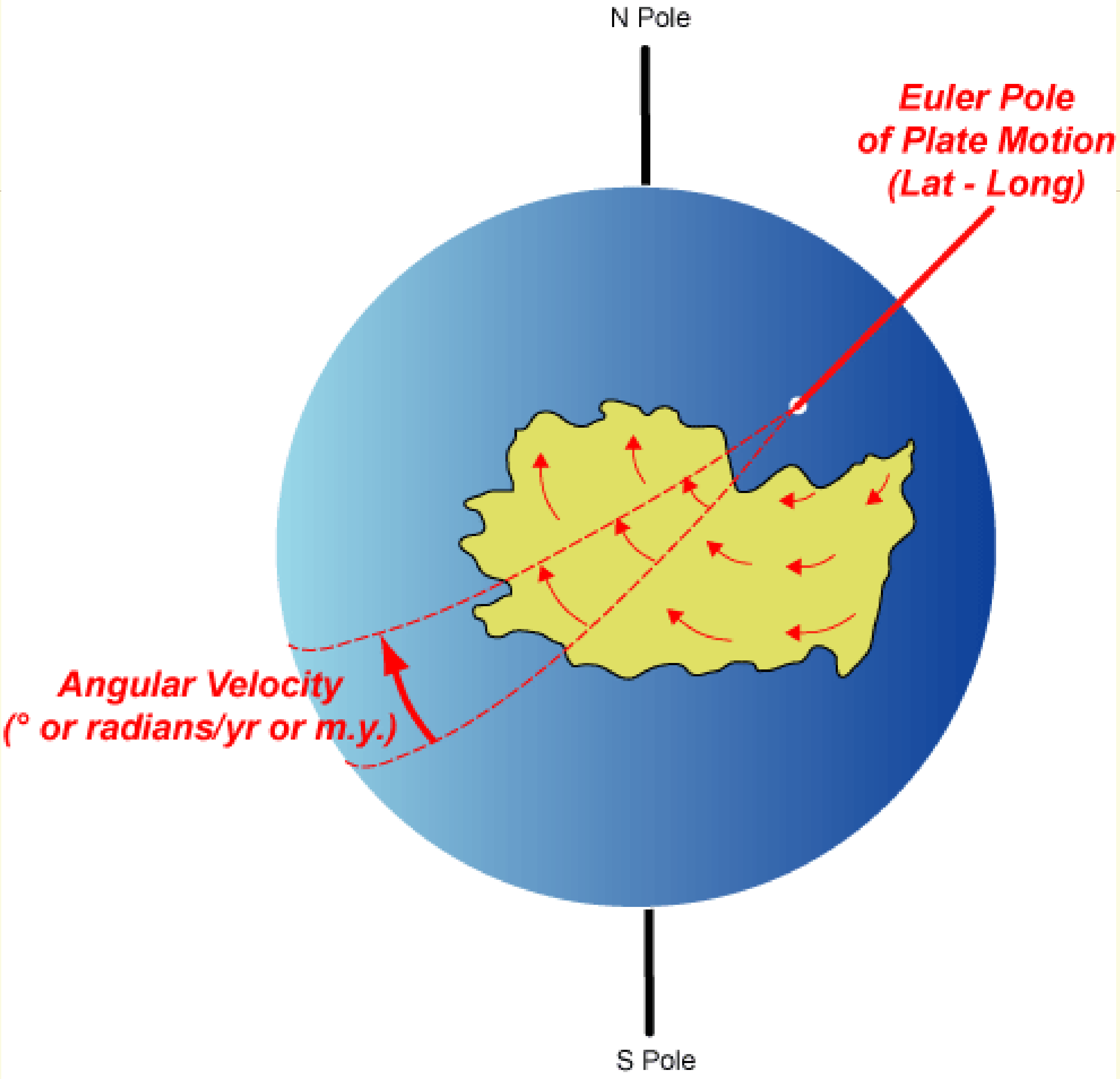
N Pole
Euler Pole
of Plate Motion
(Lat - Long)
Angular Velocity
(° or radians/yr or m.y.)
S Pole

EULER POLE FOR MOTION OF INDIA

(Ader et al, 2012)

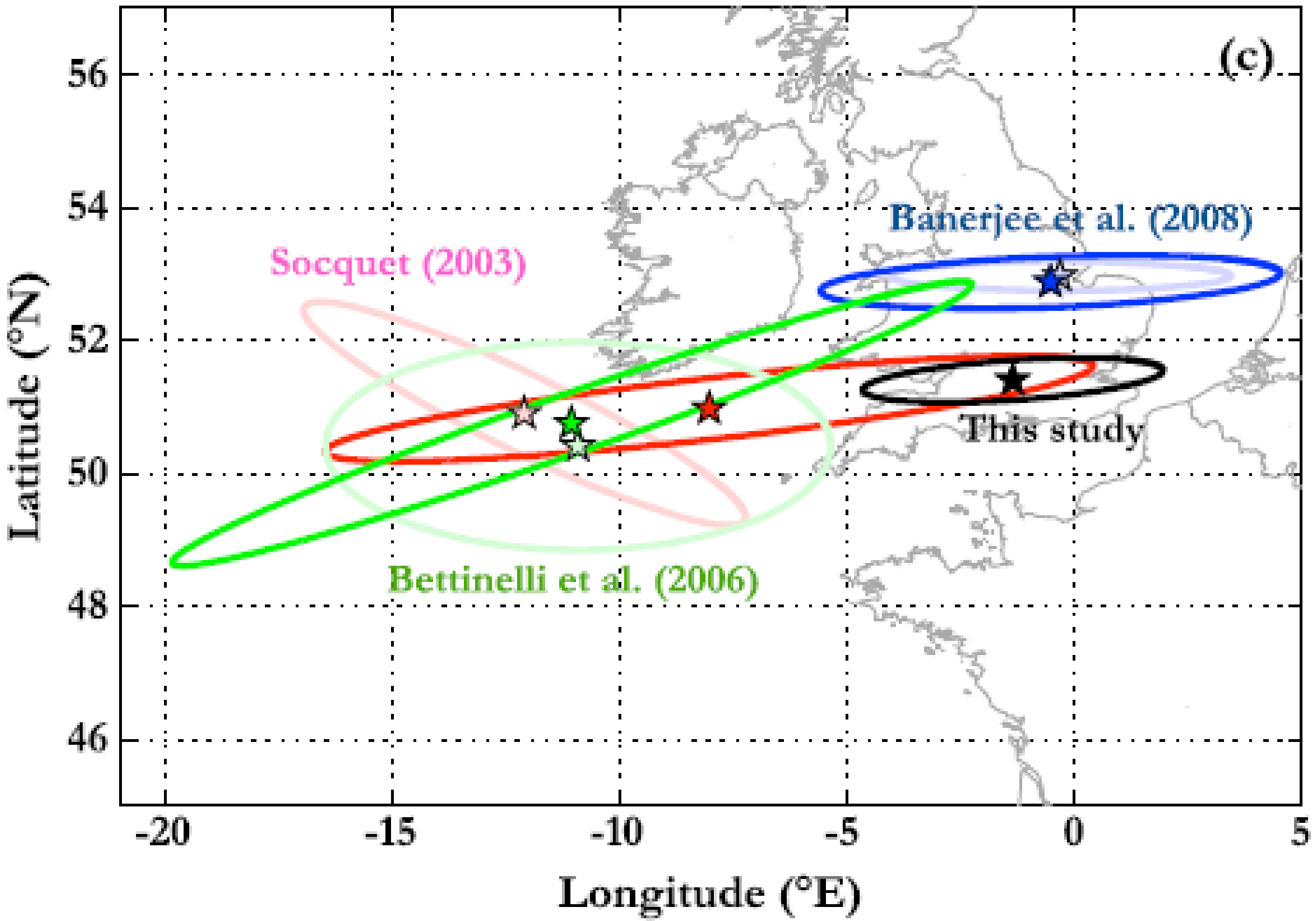

Comparison of Euler poles for Indian tectonic plate motion

Euler pole	Latitude (°)	Longitude (°)	Angular velocity (Myr^{-1})
India/ITRF2000 Present study	51.7±0.5	−15.1±1.5	0.469±0.01
India/ITRF2000 Bettinelli et al. (2006)	51.4±1.6	−10.9±5.6	0.483±0.01
India/ITRF2000 Socquet et al. (2006)	50.9±5.1	−12.1±0.6	0.486±0.01
India/ITRF1997 Sella et al. (2002)	53.7	−13.9	0.483
India/ITRF2000 SOPAC Website	53.1	2.2	0.519±0.019
India/Eurasia Present study	24.9±0.5	11.4±1.0	0.341±0.005
India/Eurasia Bettinelli et al. (2006)	26.5±3.4	13.9±7.8	0.354±0.015
India/Eurasia Socquet et al. (2006)	27.5	12.9	0.398
India/Eurasia Sella et al. (2002)	28.6±1.1	11.6±14.4	0.357±0.033
India/Eurasia Paul et al. (2001)	25.6±1.0	11.1±9.0	0.44±0.026

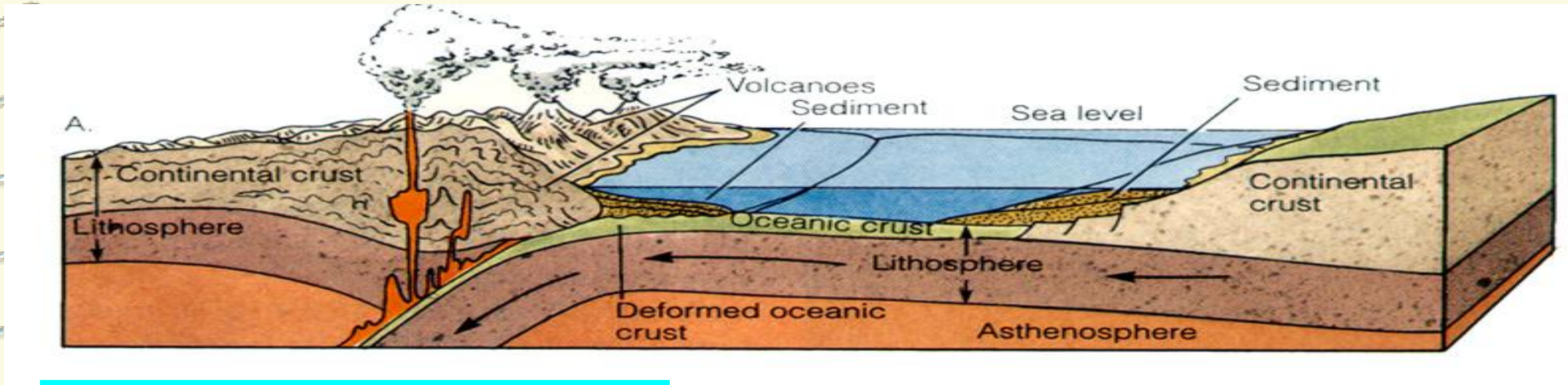

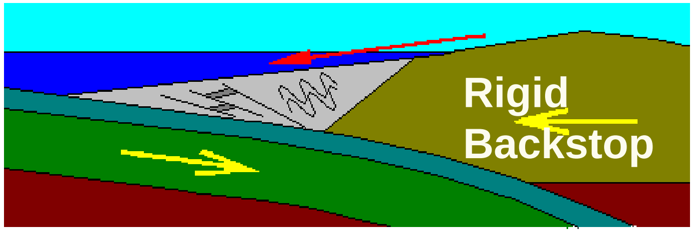

COLLISION RESULTED IN HIMALAYA

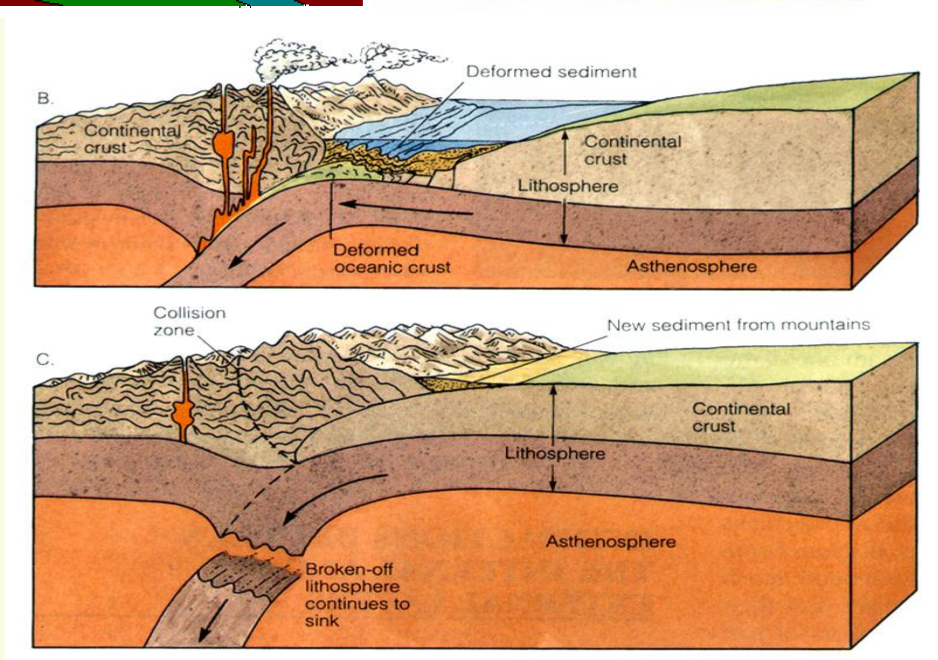

HIMALAYAN ARC

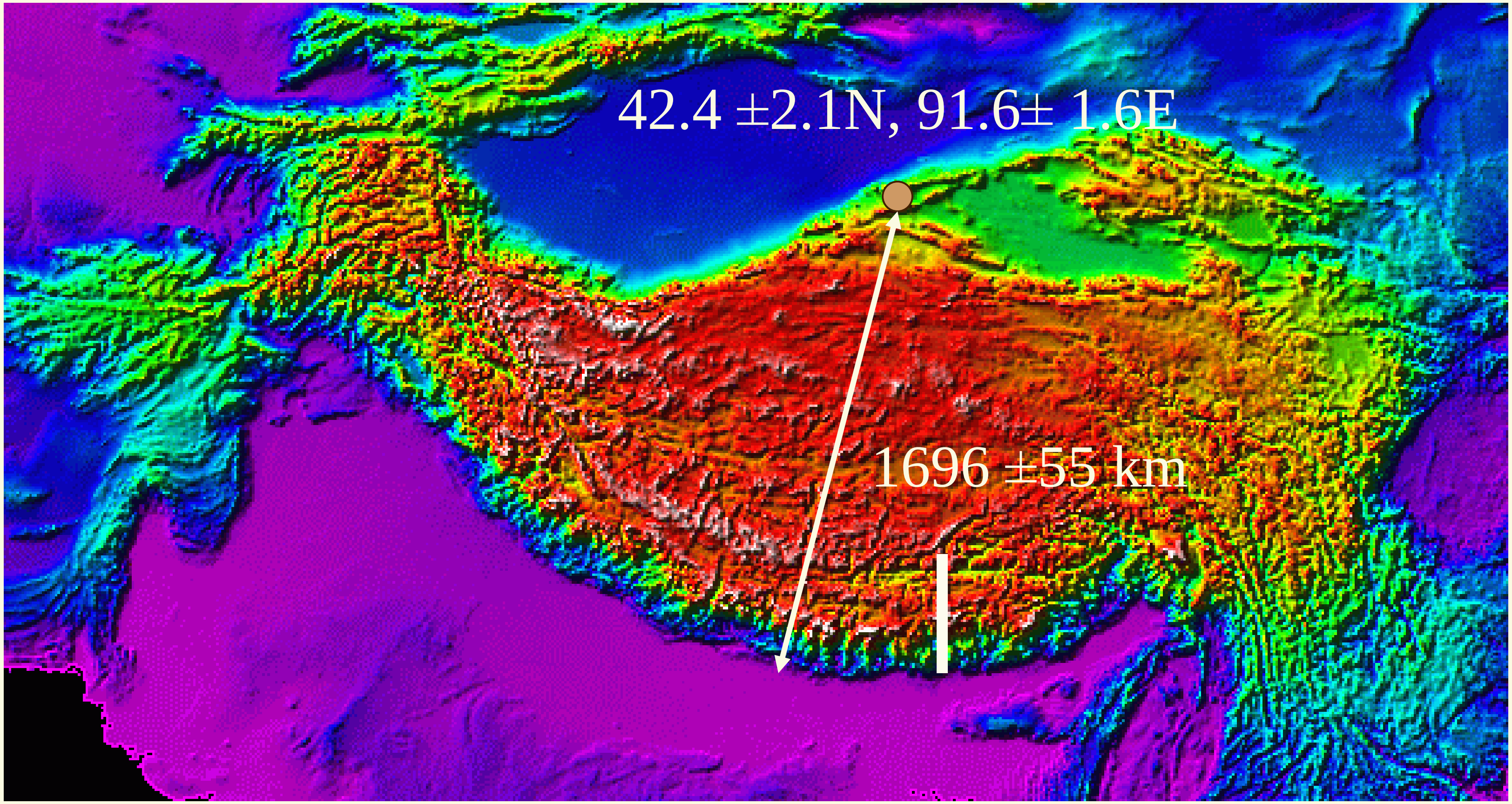

http://www.geo.cornell.edu/grads/duncan/topo/topo.gif
(Bendick and Bilham, Geology, 2001)

HIMALAYA IN CROSS-SECTION

Kangmar Anticline: ~ 10 Ma

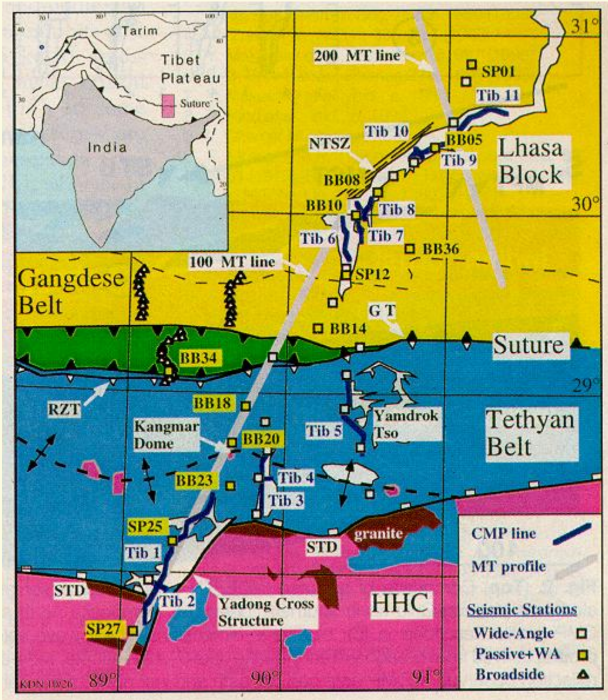

Nelson et al (1996, Science)

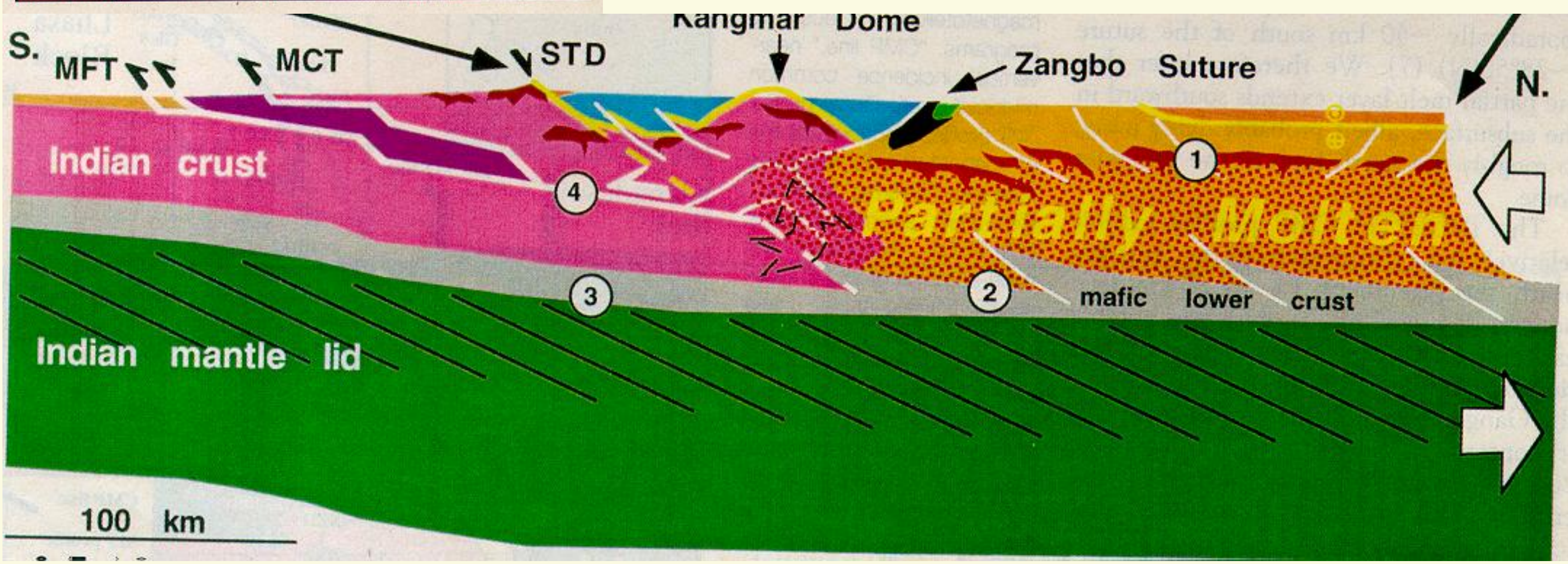

Deforming Wedge

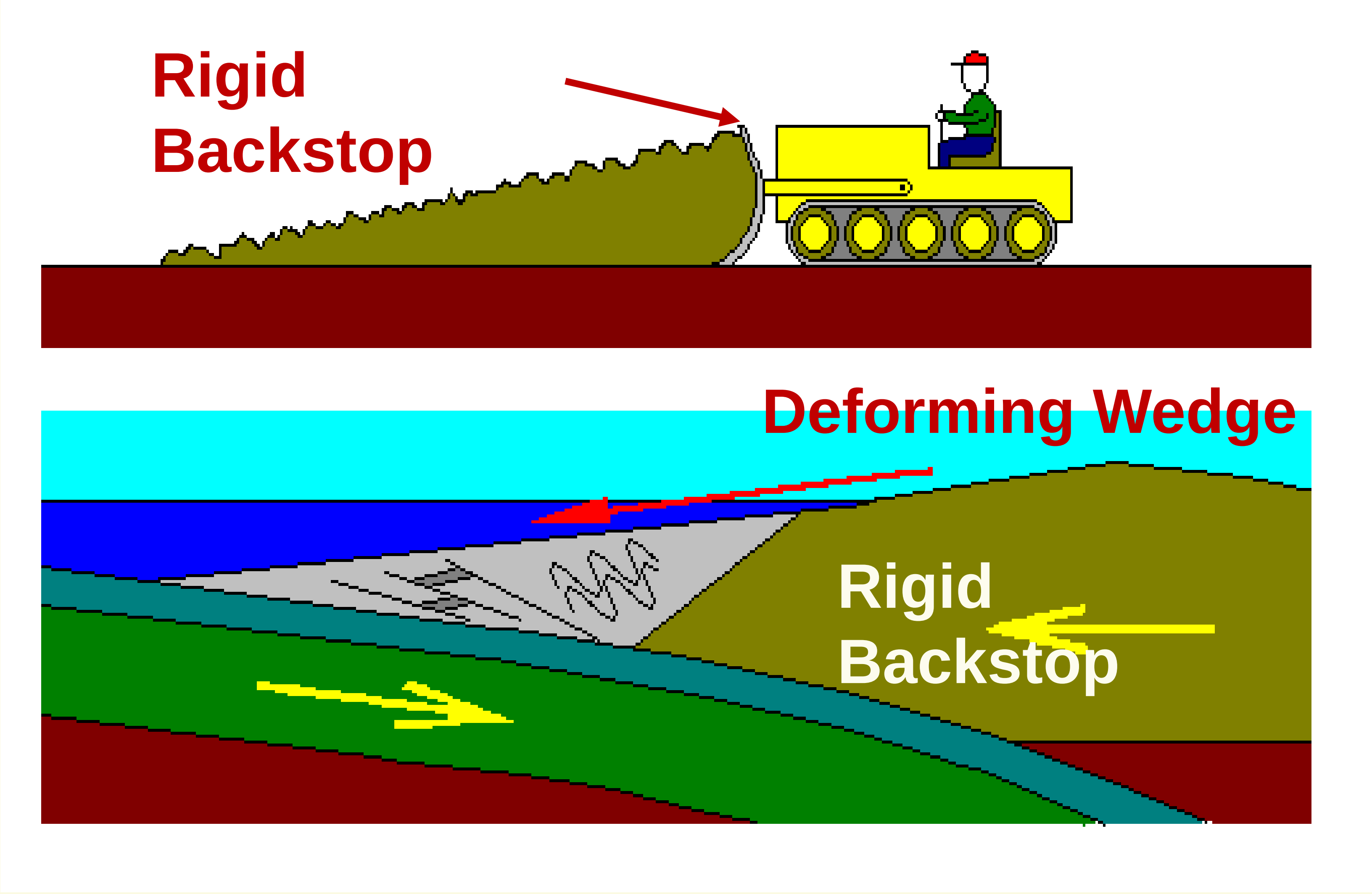

The critical taper model

"Mechanics of Fold-and-Thrust Belts and Accretionary Wedges"

Davis, Suppe & Dahlen,
JGR, 1983

Characteristics of the accretionary wedge:

- basal decollement,

- important compressive deformation above decollement, minor deformation below,

- wedge shaped.

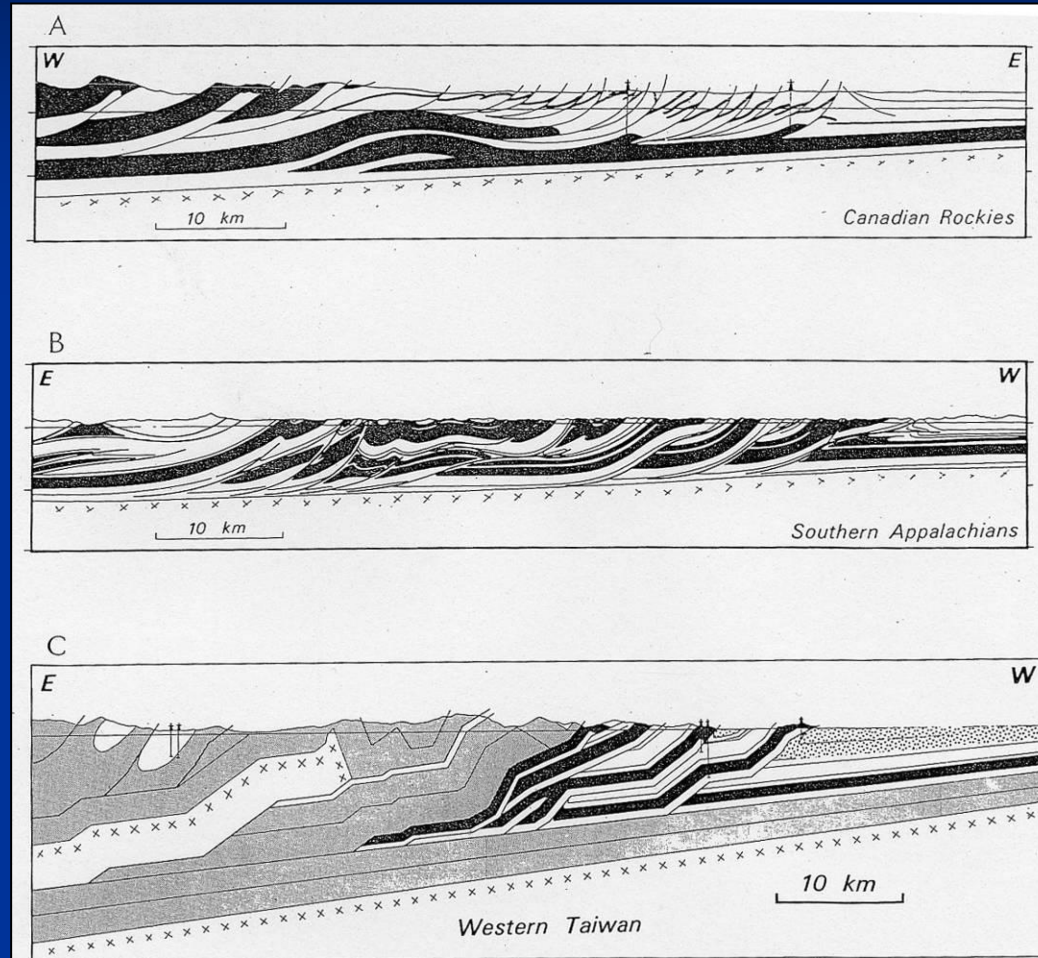

Fig. 1. Cross sections of several foreland fold-and-thrust belts: (*a*) Canadian Rockies [after *Bally et al.*, 1966], (*b*) southern Appalachians [after *Roeder et al.*, 1978], and (*c*) western Taiwan [after *Suppe*, 1980*a*].

CRITICAL WEDGE MODEL

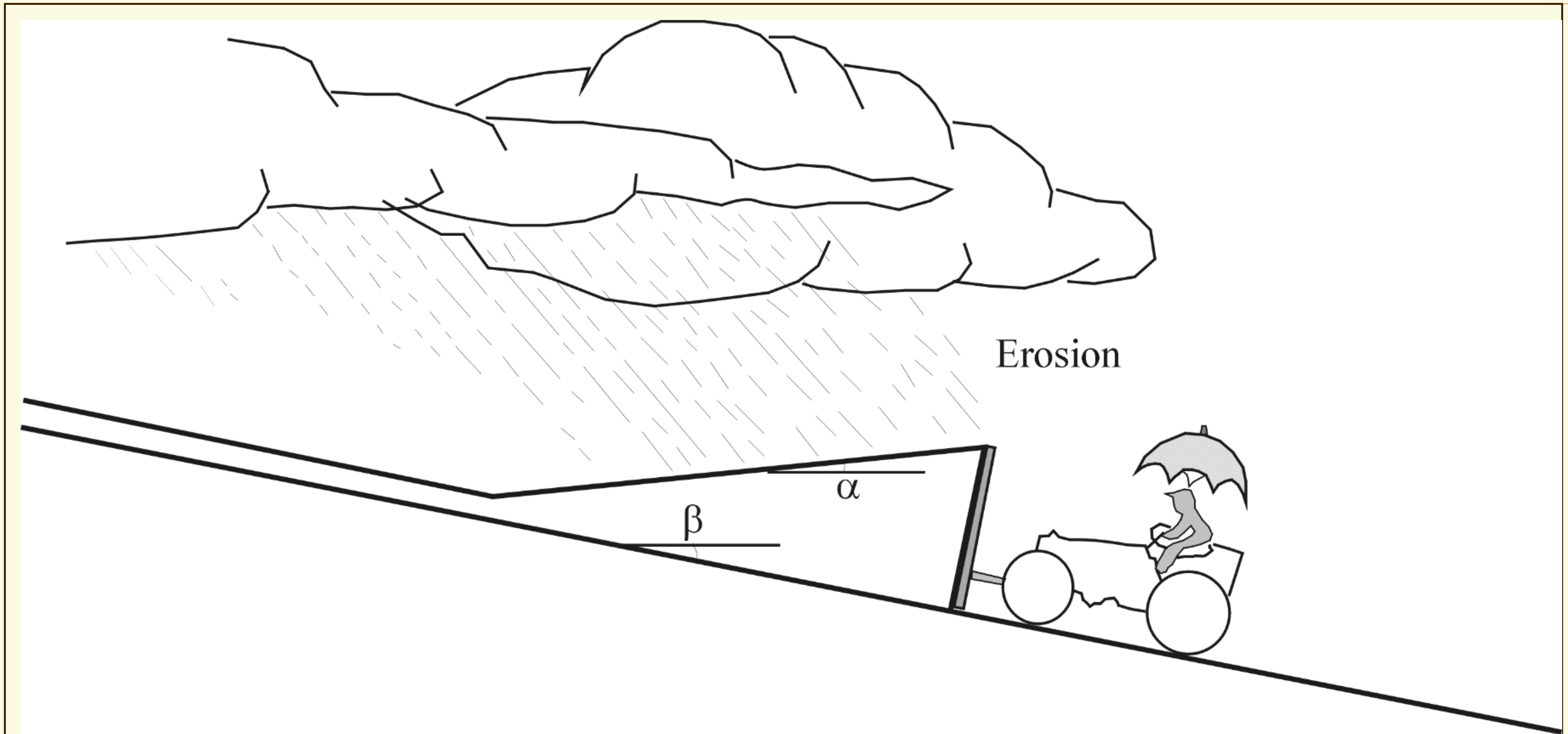

Taper (θ)= Topographic Slope (α) + Basement Slope (β)

(Davis et. al. 1983; Dahlen, 1990)

Mechanical model

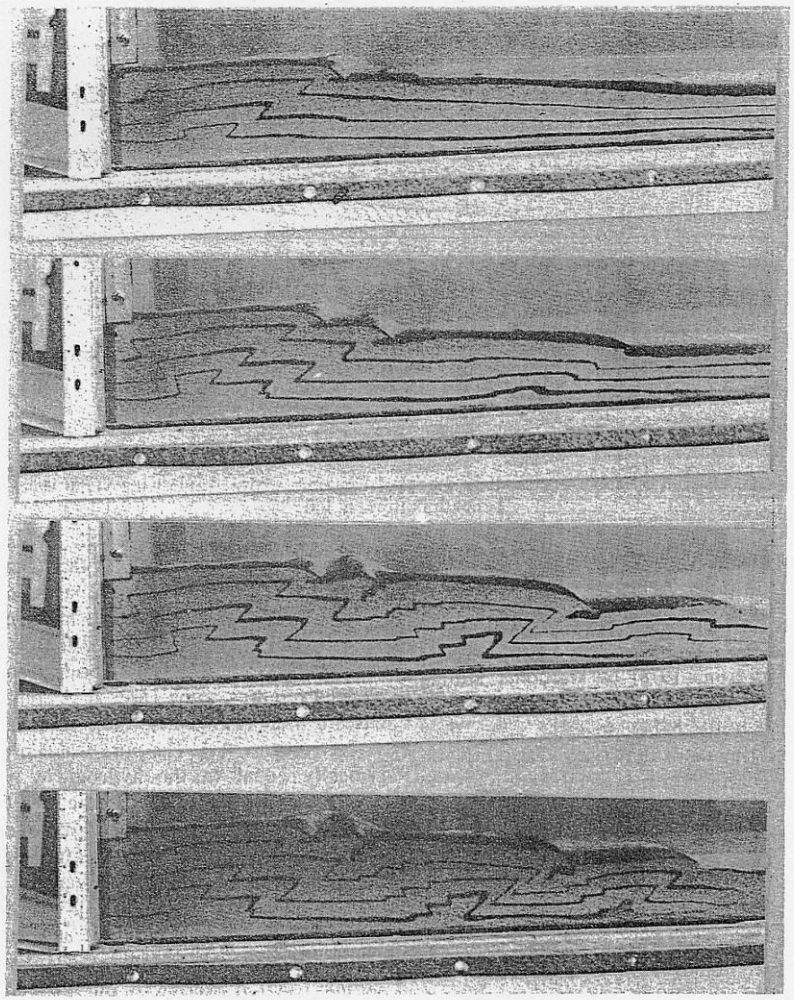

Fig. 3. Photographic side view of stages in deformation of sand during an experimental run. Initially undeformed sand mass is increasingly compressed and deformed by thrusting until the critical taper is attained. Black sand layers are passive markers.

Coulomb failure criterion :

$$\tau = S_O + \mu(\sigma_n - p_f)$$

τ = shear traction at failure,

S_0 = cohesive strength,

μ = coefficient of friction,

σ_n = normal traction,

p_f = pore fluid pressure.

The critical taper

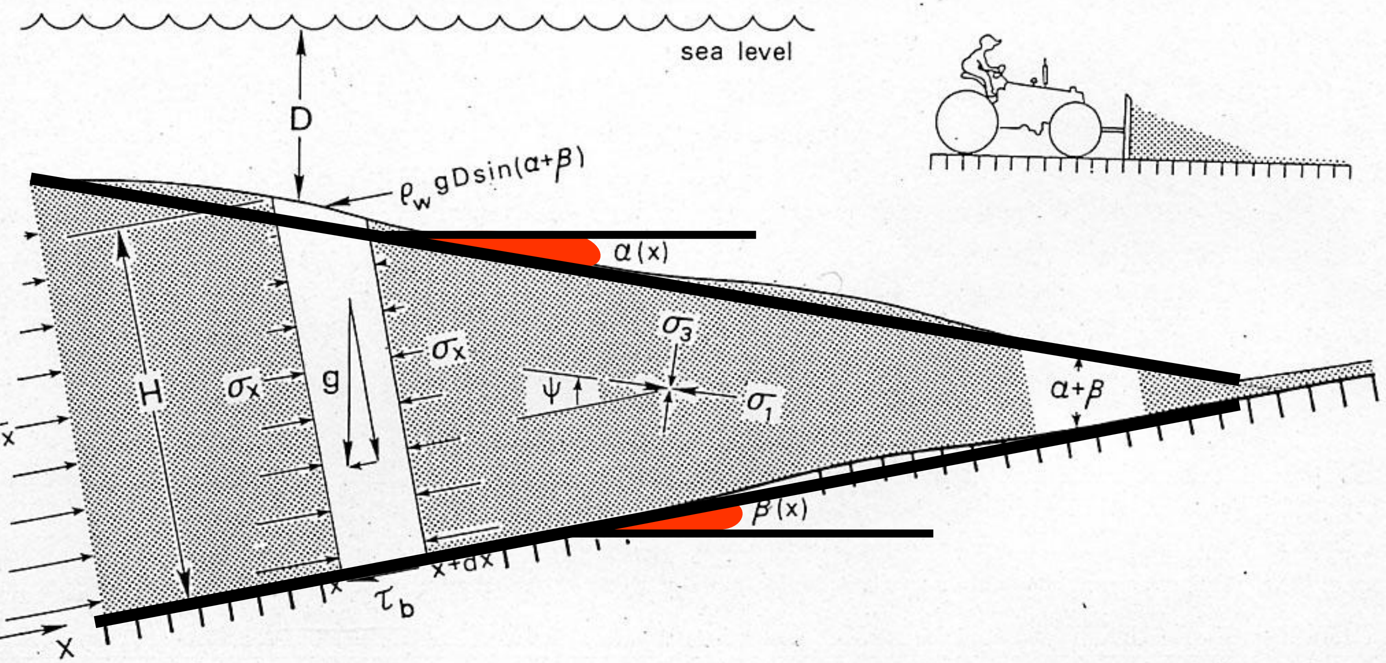

Fig. 5. Schematic diagram of a wedge of material subject to horizontal compression and on the verge of Coulomb failure throughout. The force balance on an arbitrary column of width dx is shown and the terminology used in deriving the equations of critical taper is indicated.

$$\rho g H \sin\beta + \rho_w g D \sin(\alpha+\beta) + \tau_b + \frac{d}{dx}\int_O^H \sigma_x dz = 0$$

The Mohr diagram is used to solve the equation and describe the shape of the taper

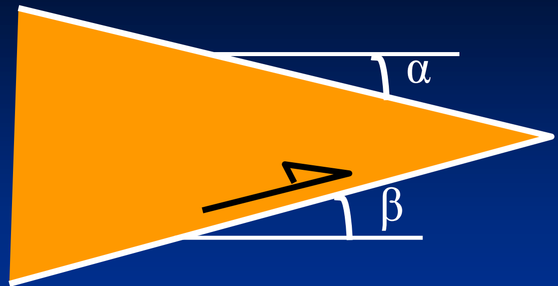

$$\alpha + \beta = f(\mu, \mu_b, \lambda)$$

where $$\lambda = \frac{p_f - \rho_w g D}{\sigma_z - \rho_w g D}$$ and μ = coefficient of friction (μ_b = basal coef.)

$$\alpha + R\beta = F$$

Linear relationship between α and β

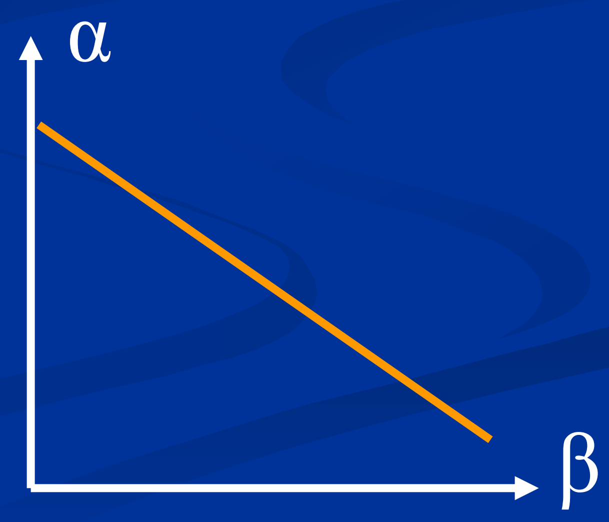

Application to natural objects: Taiwan

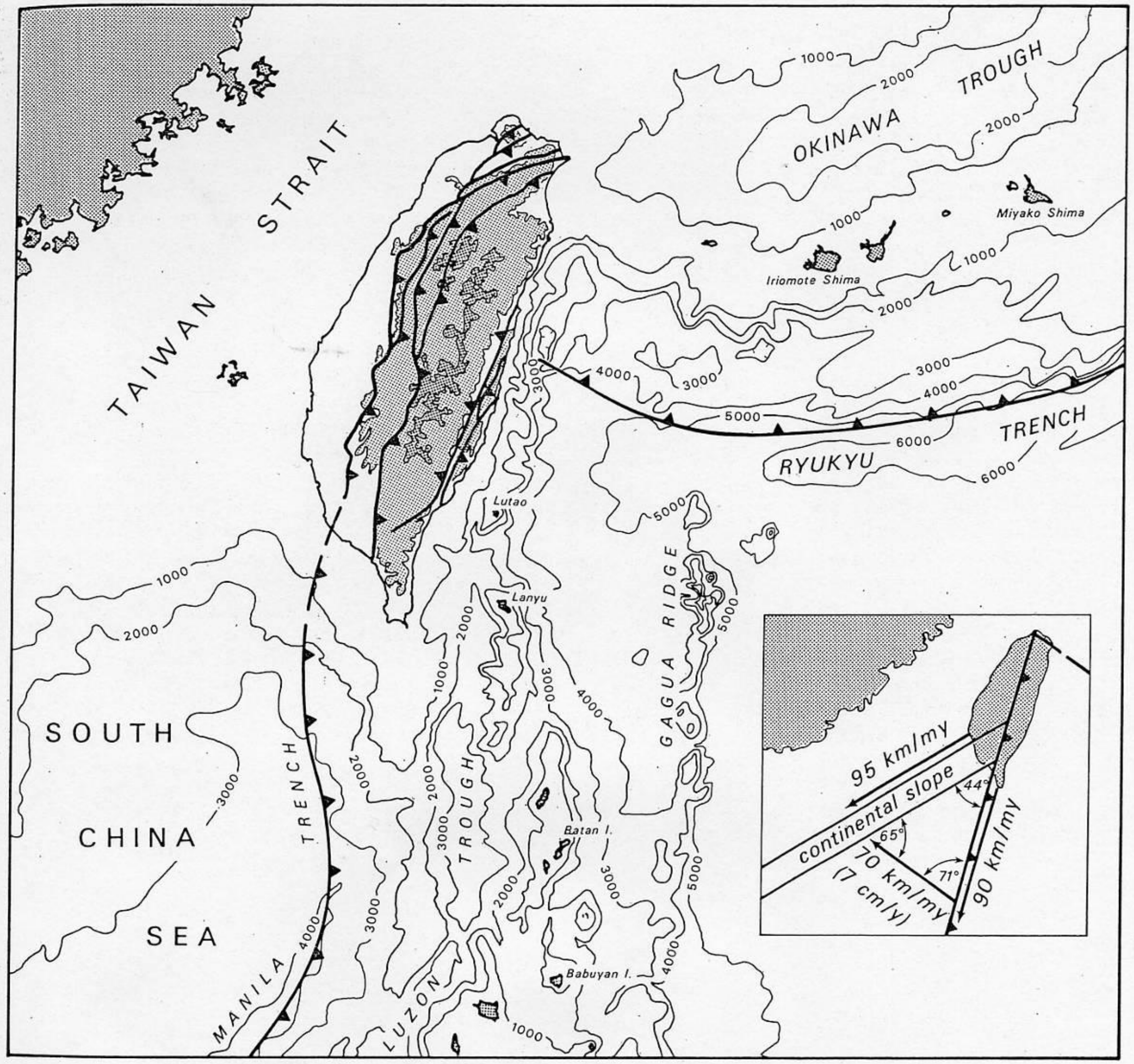

Fig. 9. Tectonic and bathymetric setting of Taiwan with velocity triangle for arc-continent collision in Taiwan assuming plate motions of *Seno* [1977].

Topographic profiles (Western Range of Taiwan): values of α

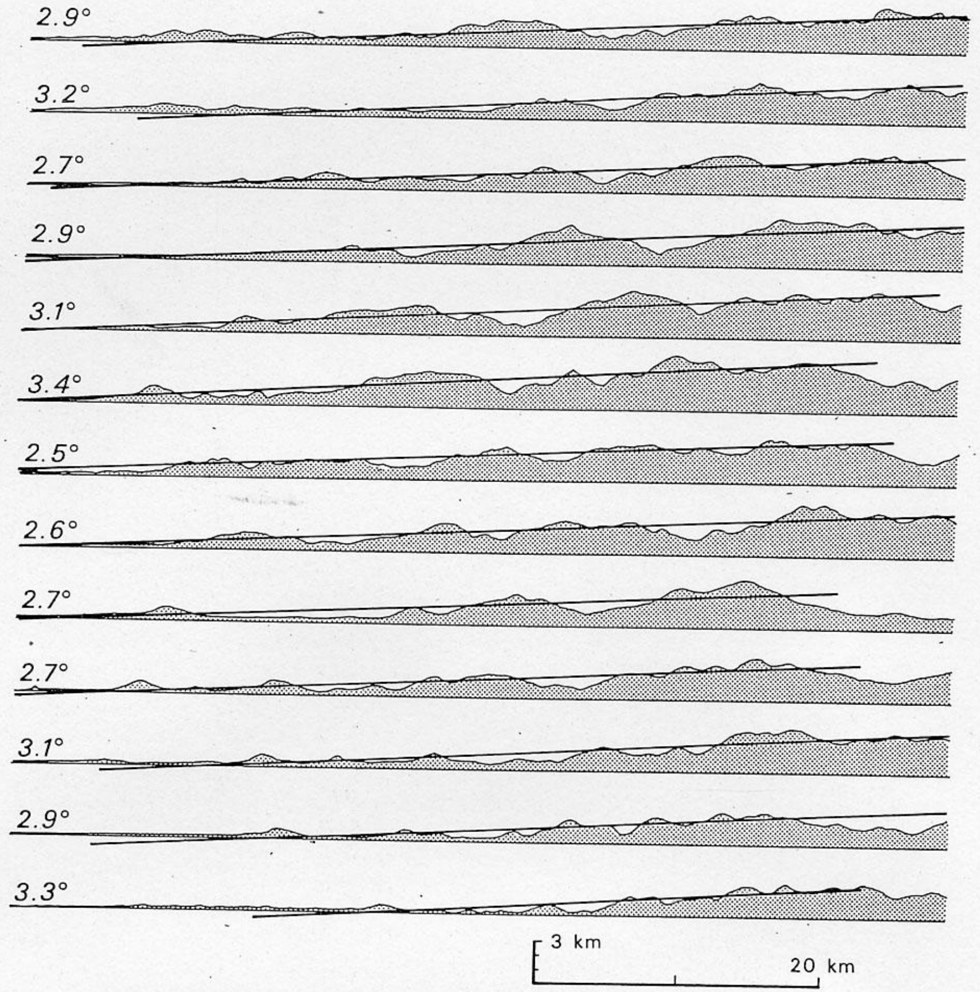

Fig. 12. Topographic profiles of western slope of central Taiwan in the region of steady state topography (see *Suppe* [1981] for locations). In all cases the topography can be well fit by a constant-slope regression. The mean slope of the set of profiles is $\alpha = 2.9° \pm 0.3°$.

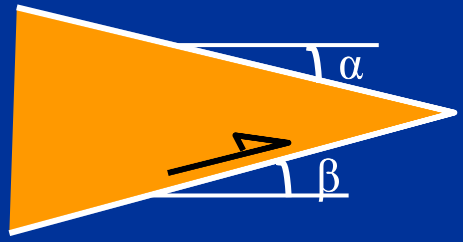

$$\alpha + \beta = f(\mu, \mu_b, \lambda)$$

Determination of the parameters producing the best fit between model and field data

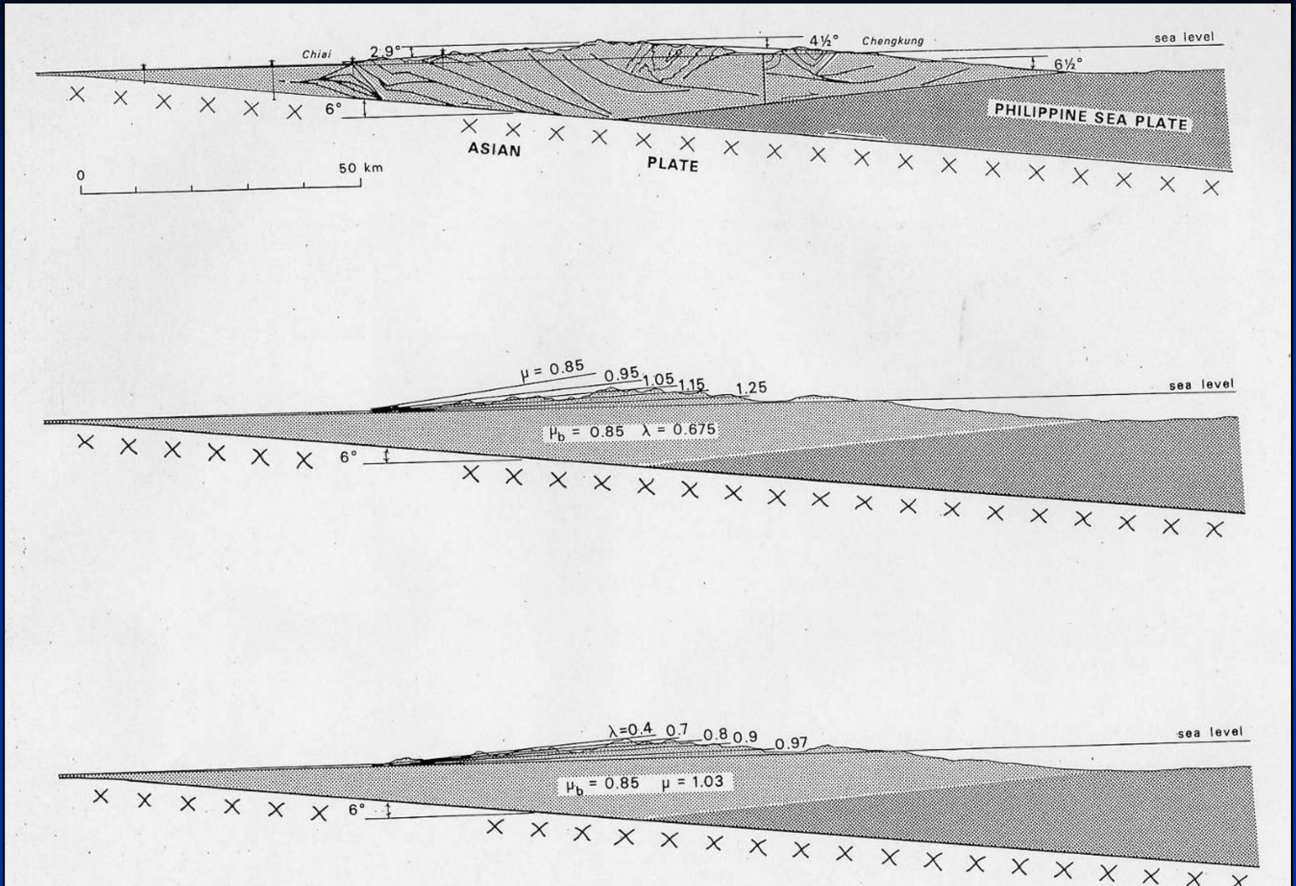

Fig. 10. Regional tectonic cross section of south-central Taiwan near Chiai oriented N20°E. Based on data of *Suppe* [1980*b*, 1981], *Stanley et al.* [1981], and *Chi et al.* [1981]. The regional surface slope of 2.9° in western Taiwan is well explained by the critical Coulomb wedge theory with $\mu_b = 0.85$, $\mu = 1.03$, and $\lambda \approx 0.7$. The sensitivity to μ with the fluid pressure ratio fixed at the observed value $\lambda = 0.675$ is greater than the sensitivity to λ for fixed μ.

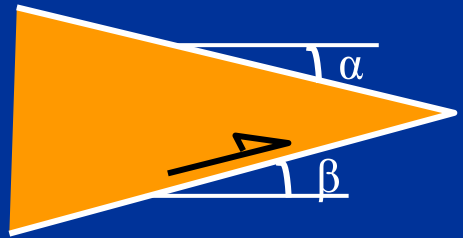

$$\alpha + \beta = f(\mu, \mu_b, \lambda)$$

Other examples: values of α and β

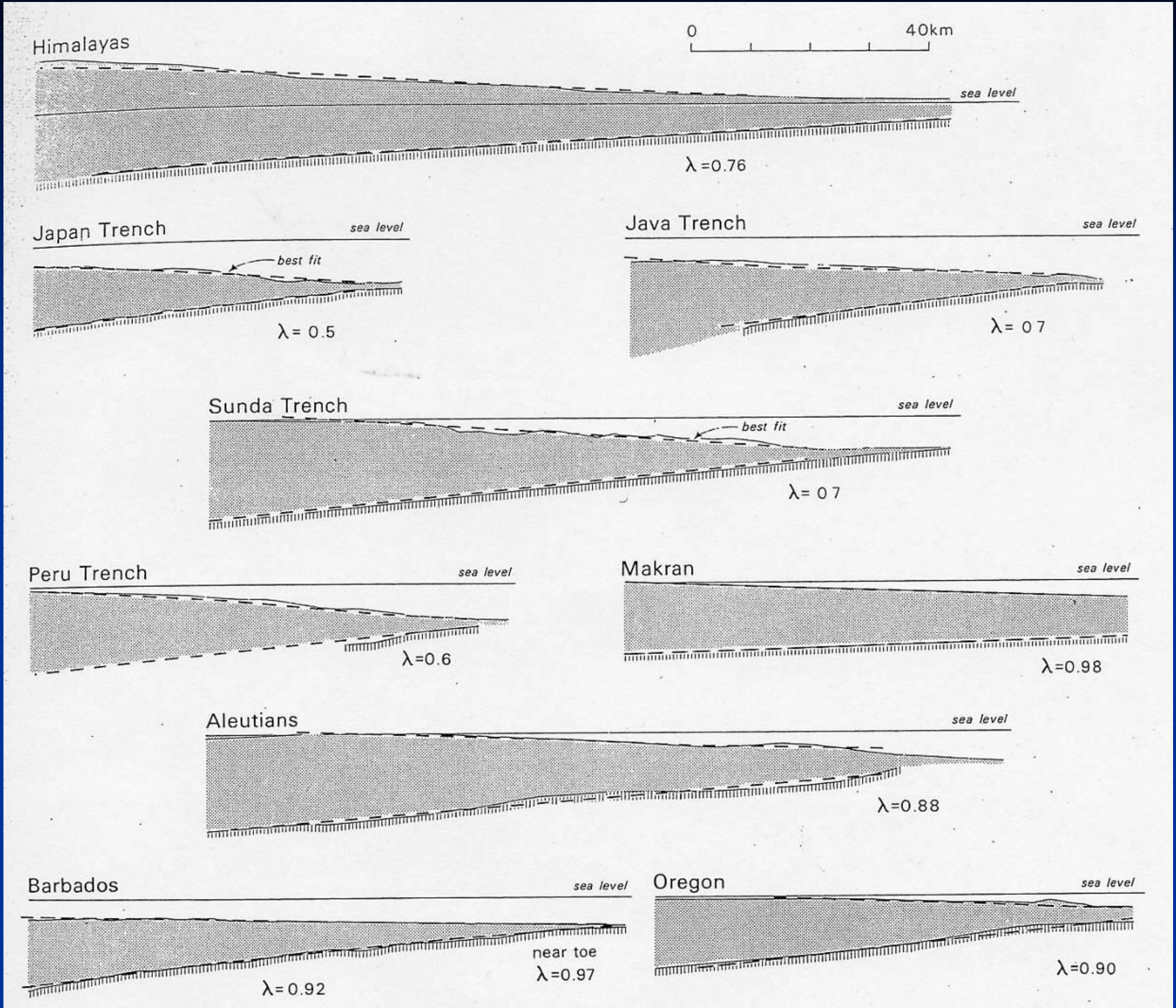

Fig. 16. Cross sections of the Himalayan fold-and-thrust belt and various active submarine accretionary wedges. Heavy dashed lines are best fitting linear profiles used to infer the fluid pressure ratios $\lambda = \lambda_b$, which are also shown.

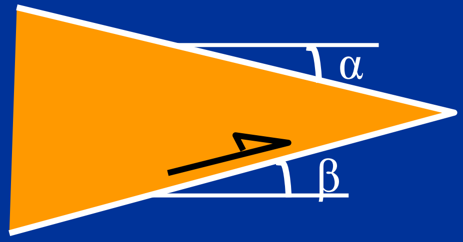

$$\alpha + \beta = f(\mu, \mu_b, \lambda)$$

Constraining the parameters

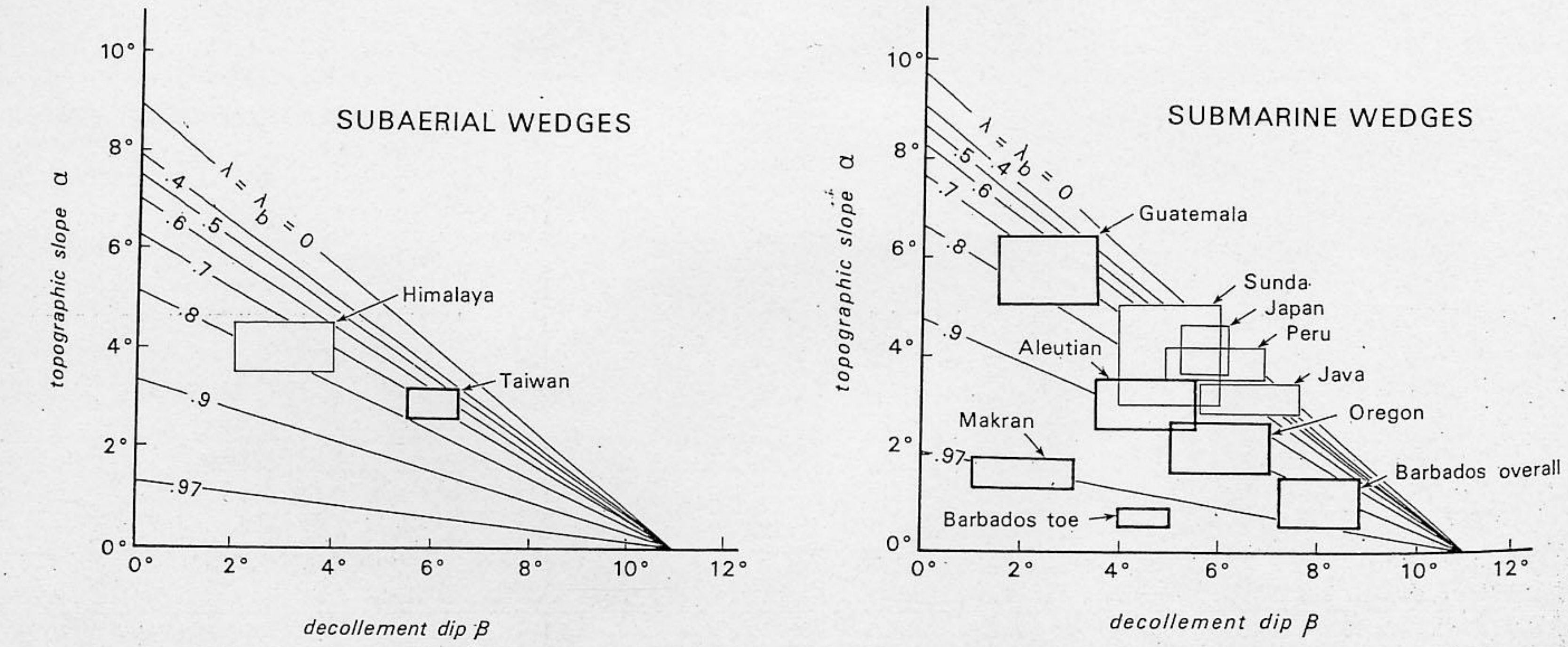

Fig. 17. Theoretical linear relationships $\alpha + R\beta = F$ for various fluid pressure ratios $\lambda = \lambda_b$, assuming $\mu_b = 0.85$ and $\mu = 1.03$. Boxes indicate observed geometries of active wedges, used to infer the fluid pressure ratios within them. Heavy outlines indicate those wedges for which some direct fluid pressure information is available. A rock density $\rho = 2.4\ g/cm^3$ was used in the submarine case; other values would yield very similar results as the sensitivity to ρ is slight.

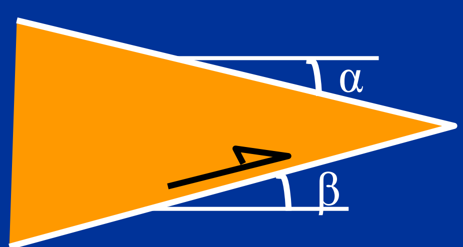

$$\alpha + \beta = f(\mu, \mu_b, \lambda)$$

$$\alpha + R\beta = F$$

Linear relationship between α and β

Modification of the equilibrium

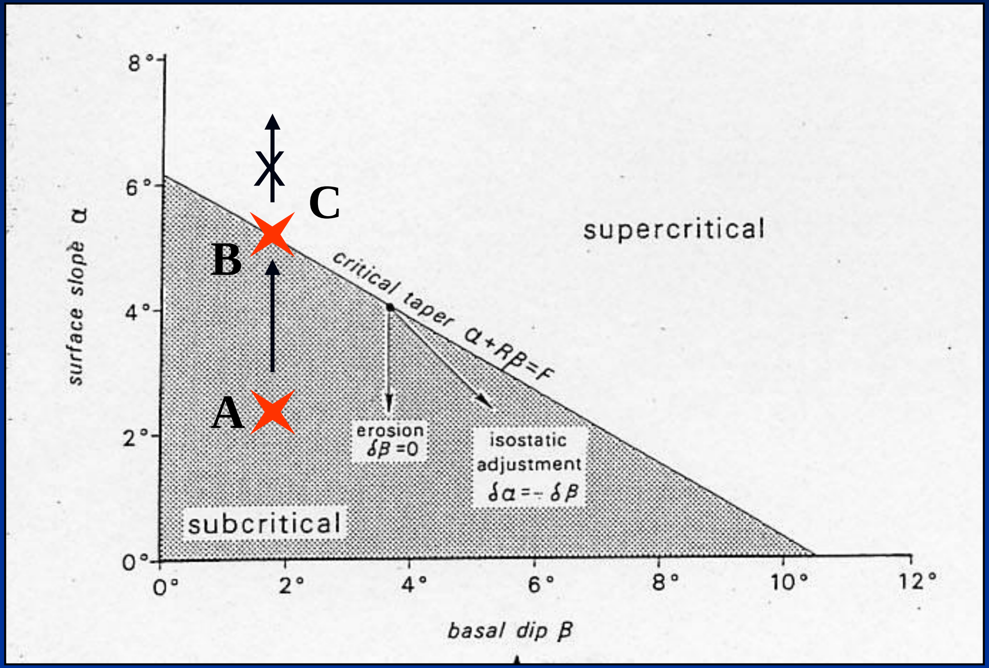

Example: mountain building

A: subcritical / “stable” → α can increase.

B: critical taper. α cannot increase anymore. If α > critical value, the taper becomes supercritical / unstable and collapses.

C: to carry on growing, the taper cannot steepen anymore so it has to “expand” horizontally as well as vertically.

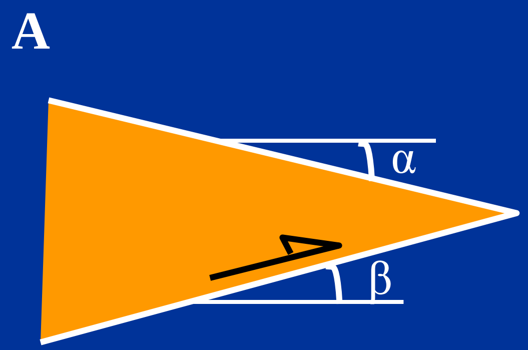

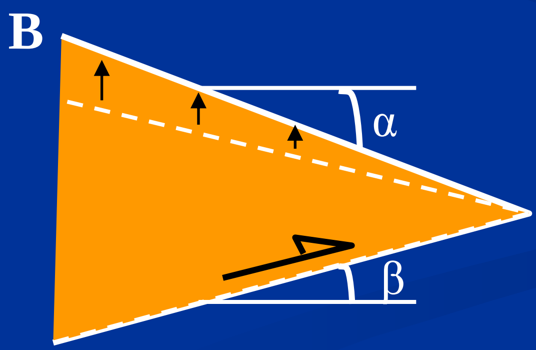

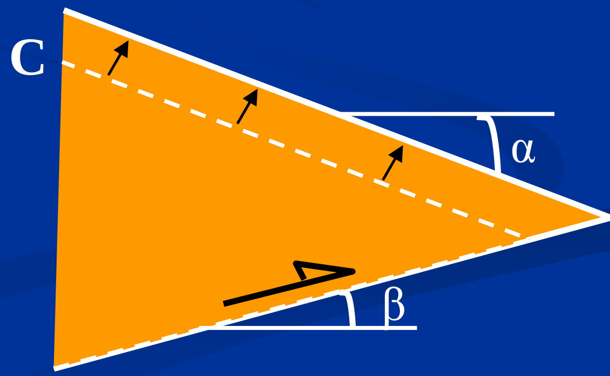

Erosion controls the geometry of mountains?

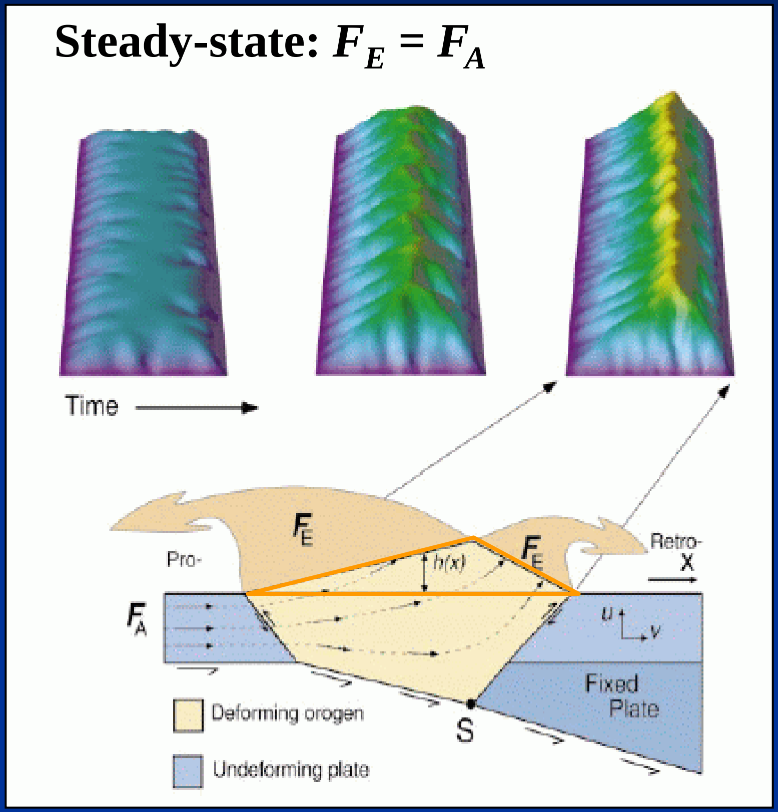

Willett & Brandon, Geology, 2002

F_A = flux of material accreted,

F_E = flux of material eroded.

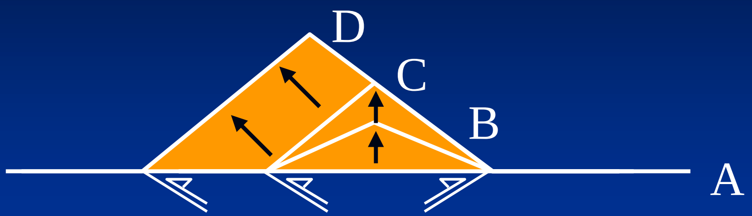

A: no topography, $F_E = 0$.
B: mountain grows → F_E increases.
C: critical taper stage, slope α cannot increase anymore.
D: $F_A = F_E$ → steady-state. The topography does not evolve anymore.

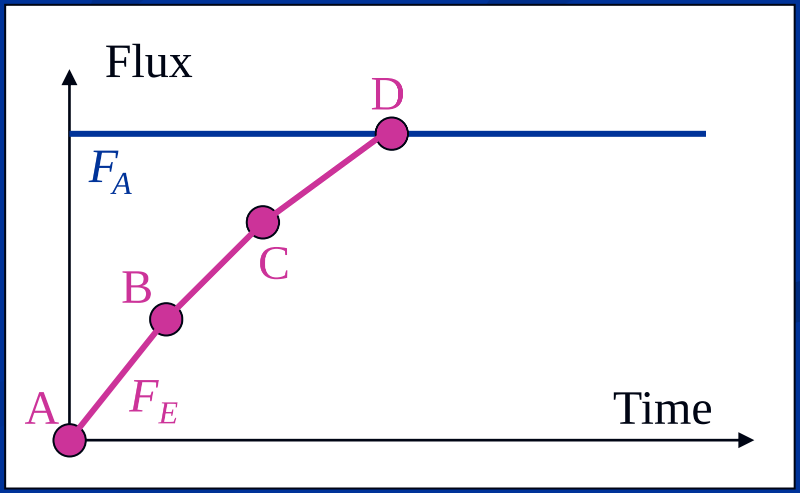

Erosion controls the geometry of mountains?

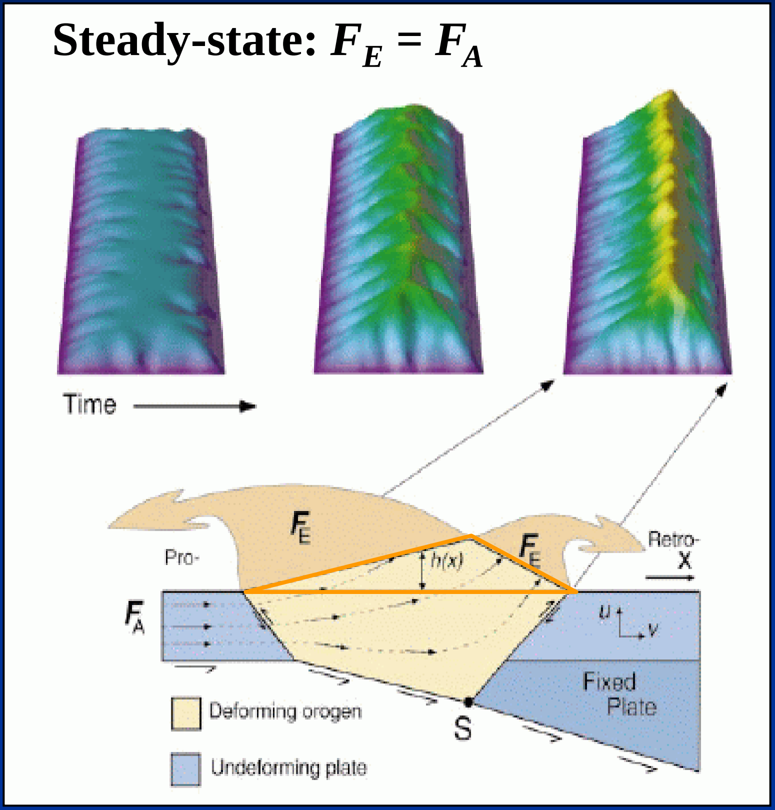

Willett & Brandon, Geology, 2002

F_A = flux of material accreted,

F_E = flux of material eroded.

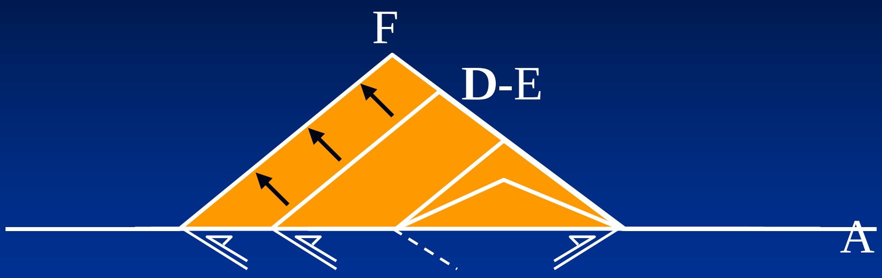

D: $F_A = F_E$ → steady-state.

E: drop in F_E (e.g., climate change with less rain) → erosion rate decreases → the topography is not at steady-state anymore.

F: mountain grows again → F_E increases until a new steady-state is reached ($F_A = F_E$)

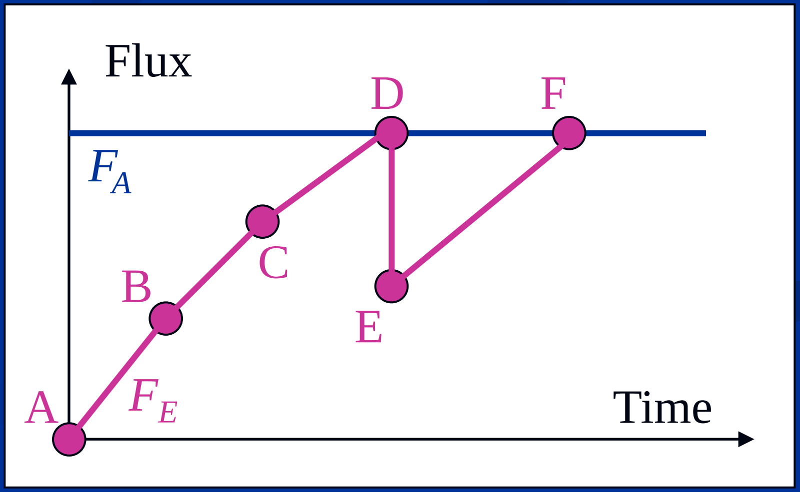

Erosion controls the geometry of mountains?

Steady-state: $F_E = F_A$

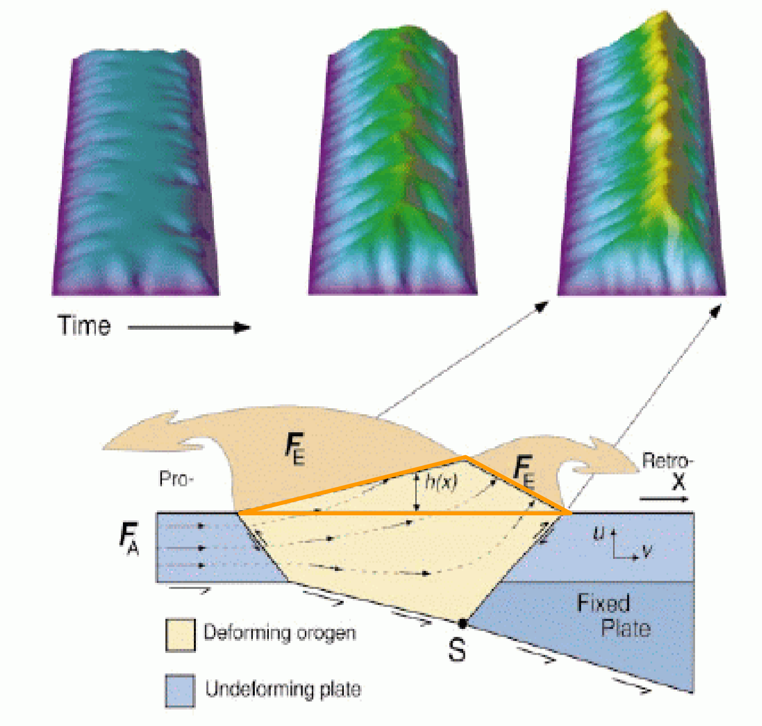

Willett & Brandon, Geology, 2002

F_A = flux of material accreted,

F_E = flux of material eroded.

→ Erosion controls the GEOMETRY of the mountain range

Remark: “real” mountains are more complex:

- presence of discontinuities (e.g. faults),

- different lithologies (more resistant in the core of the range),

- change in crust rheology (e.g. lower crust partially molten under Tibet → no basal friction).

SYMPTOMATIC APPROACH

- Mountain belts have a wedge shaped geometry since they develop from a wedge shaped sedimentary prism
- Mechanics analogous to a wedge of sand in front of a moving bulldozer
- Orogenic wedges require development of critical taper (θ_c) before they can move
- Taper given by sum of basal slope (β) and surface slope (α)

Applicability to MOUNTAIN Belts

- Wedge taper (θ) sum of the surface slope (α) and the basement dip (β)
- Wedge needs to form taper (θ) toward their undeformed foreland; moves only when a critical value (θ_c) is reached
- If (θ) < (θ_c) wedge must shorten and thicken
- If (θ) >(θ_c) wedge lengthen itself by imbrication into the undeformed foreland to reduce (θ).

CRITICAL WEDGE MODEL

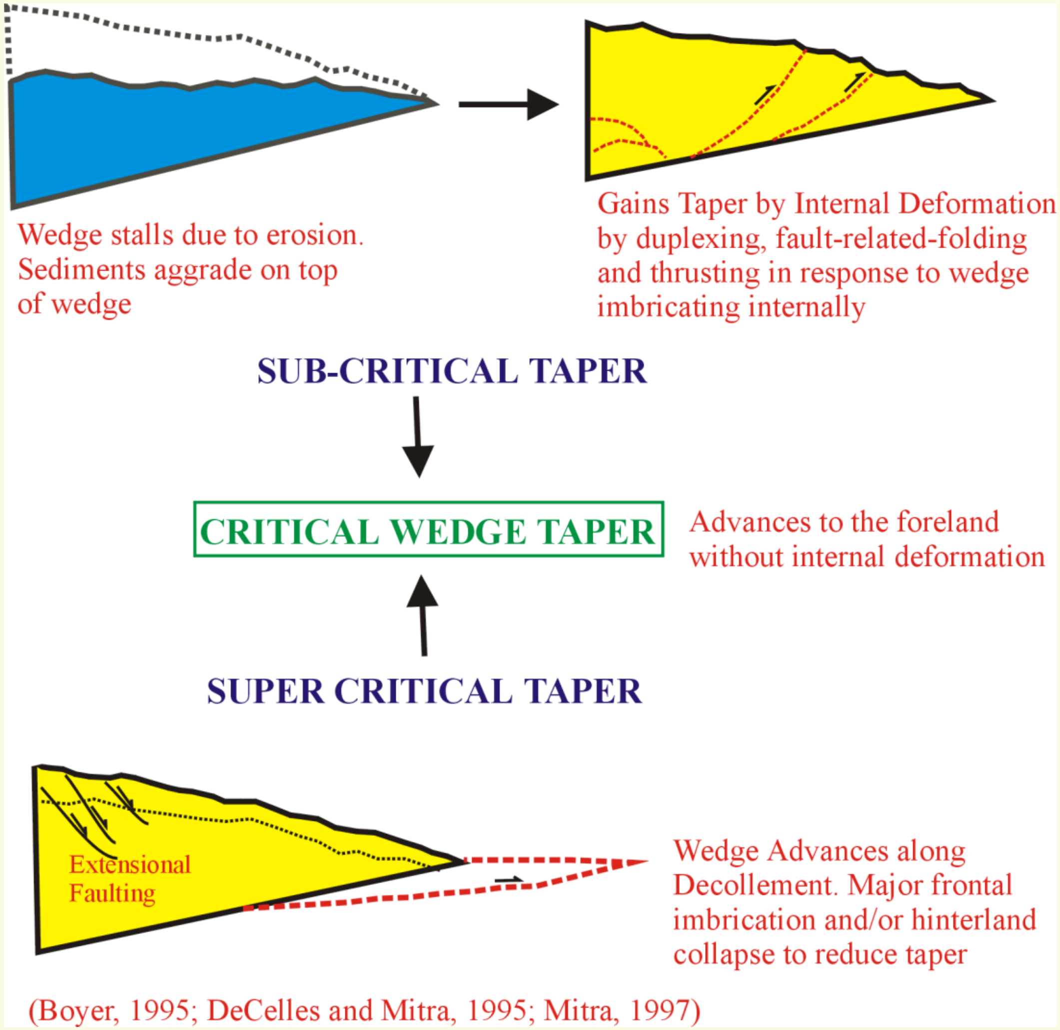

Kinematic Evolution

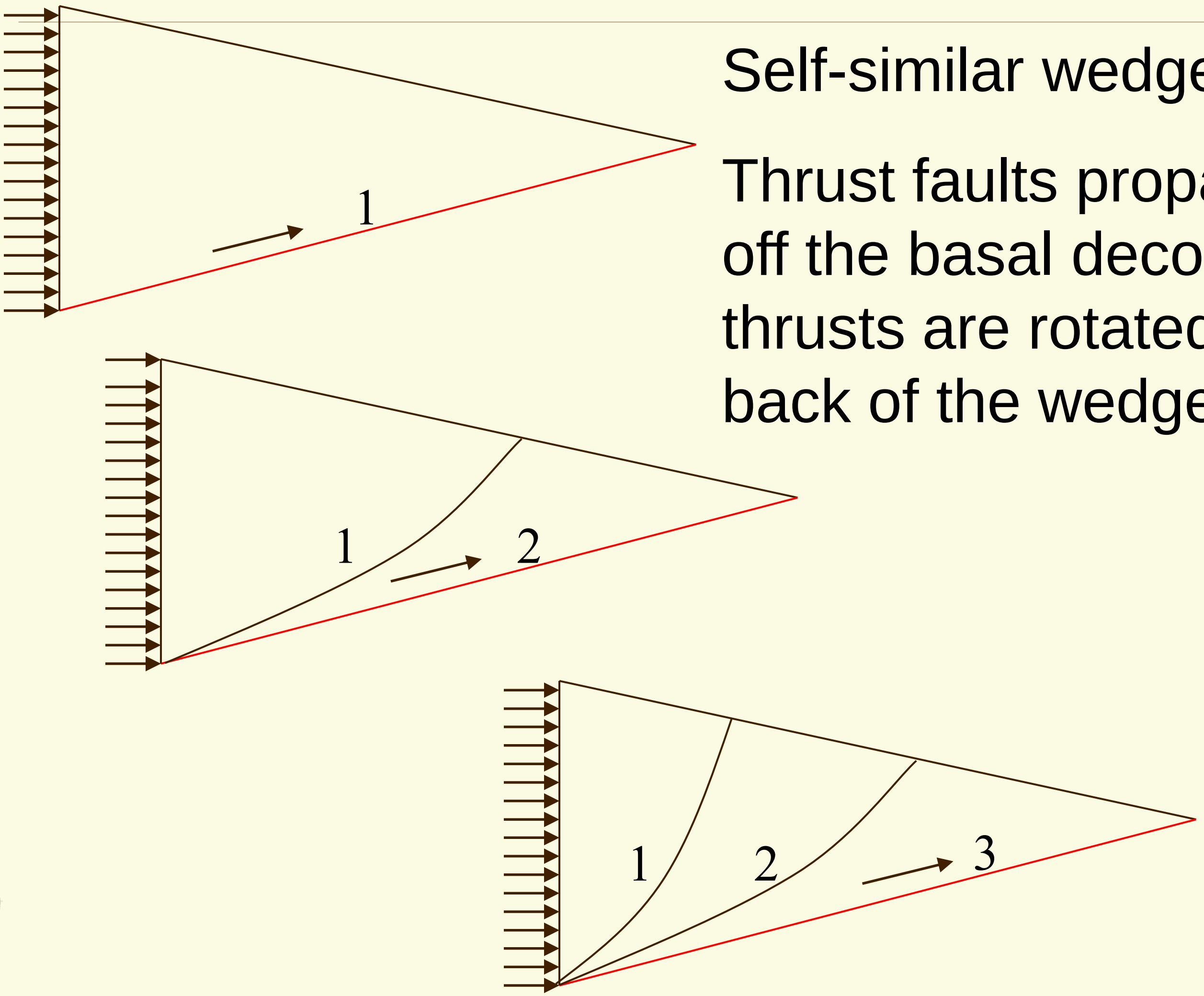

Self-similar wedge

Thrust faults propagate forward off the basal decollement. Old thrusts are rotated towards the back of the wedge

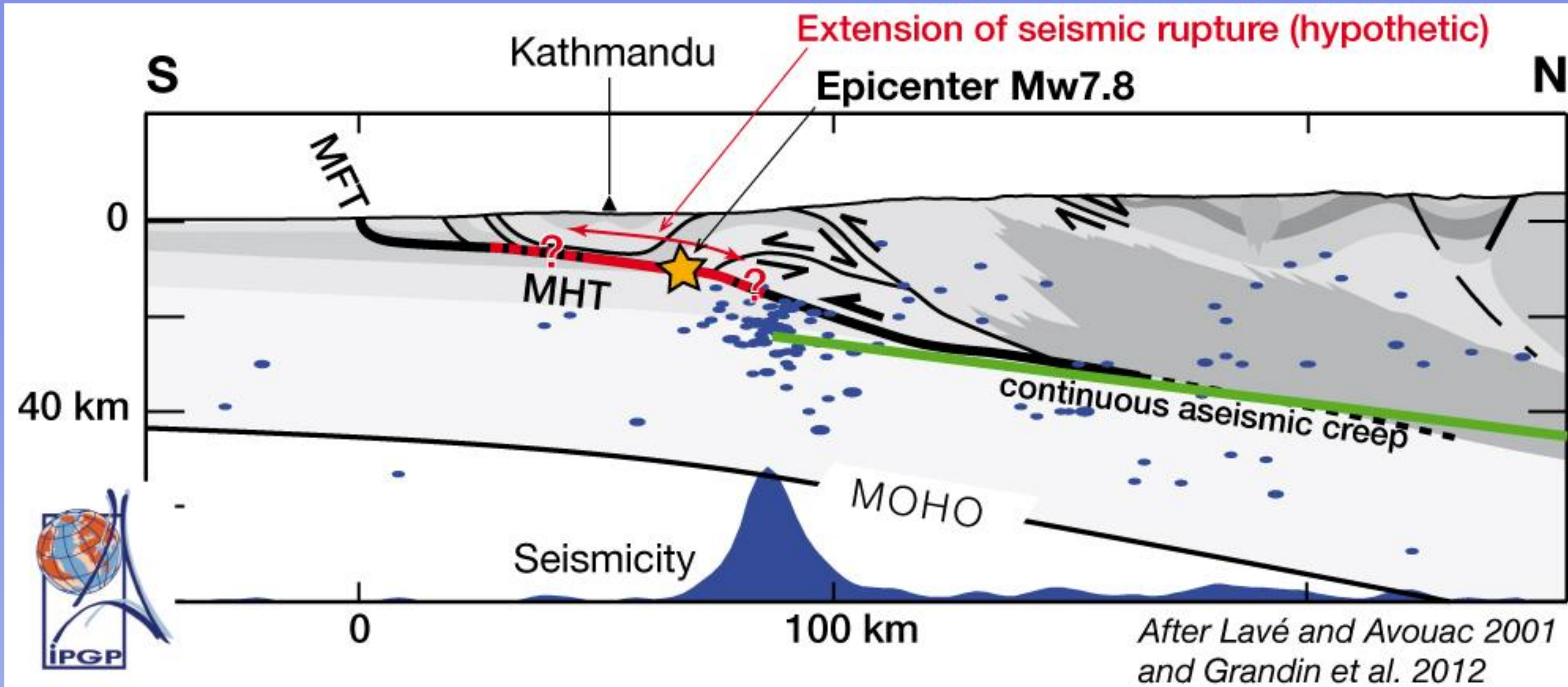

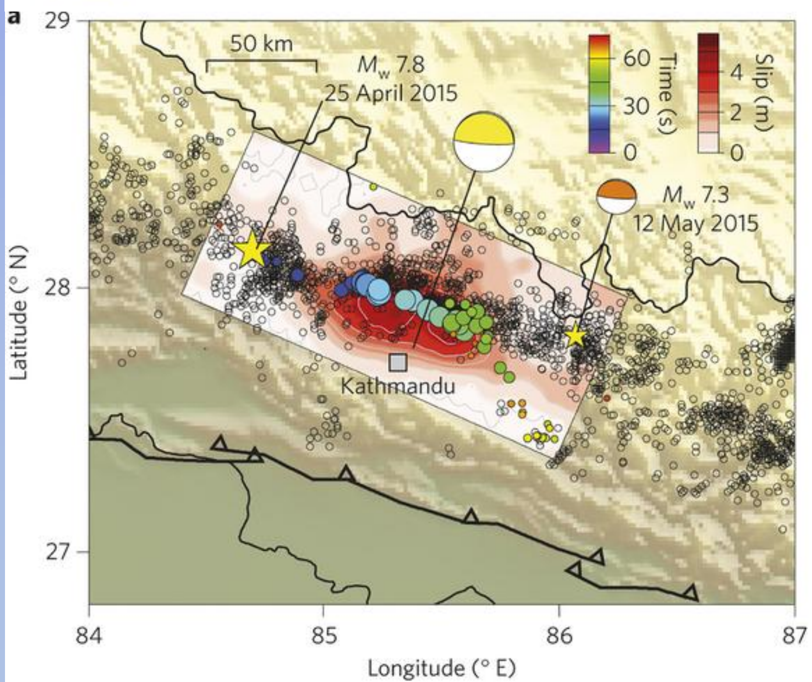

NEPAL 2015 GURKHA EARTHQUAKE

Avouac et al (2015, Nature Geoscience)

CRITICAL WEDGE MODEL

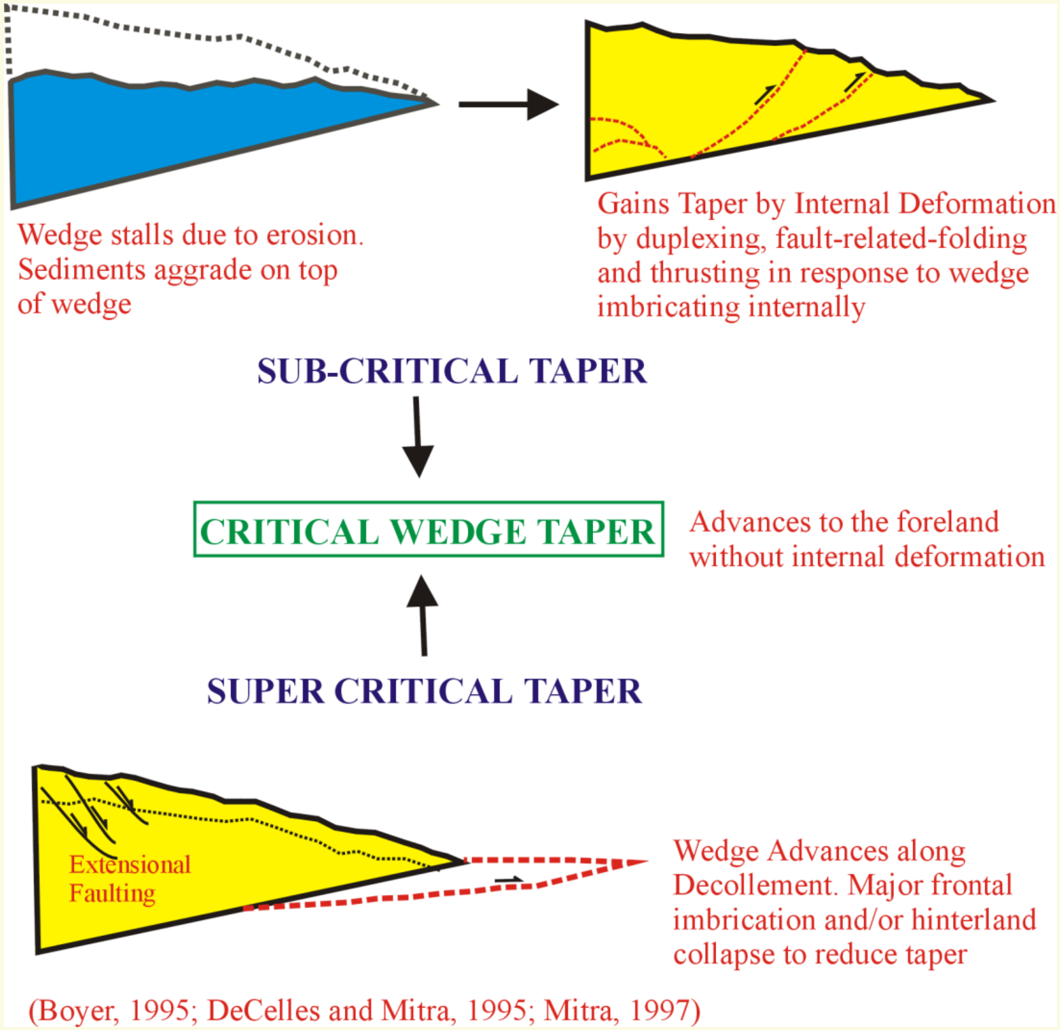

IN-SEQUENCE THRUSTING

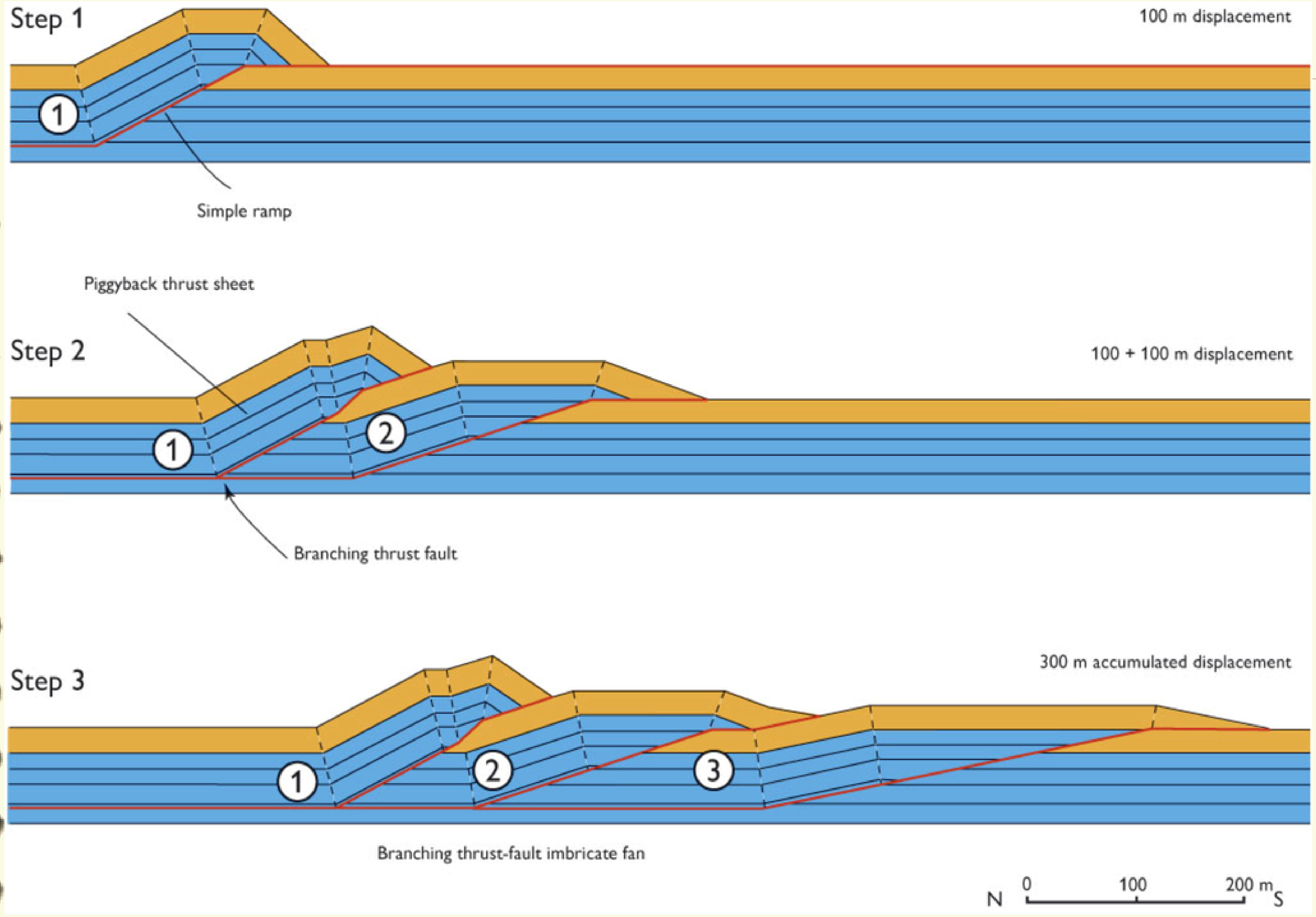

Complicated Kinematic Evolution

Subcritical wedges will deform internally to achieve critical taper.
Types of internal deformation include:

- -Backthrusting
- -Duplexes

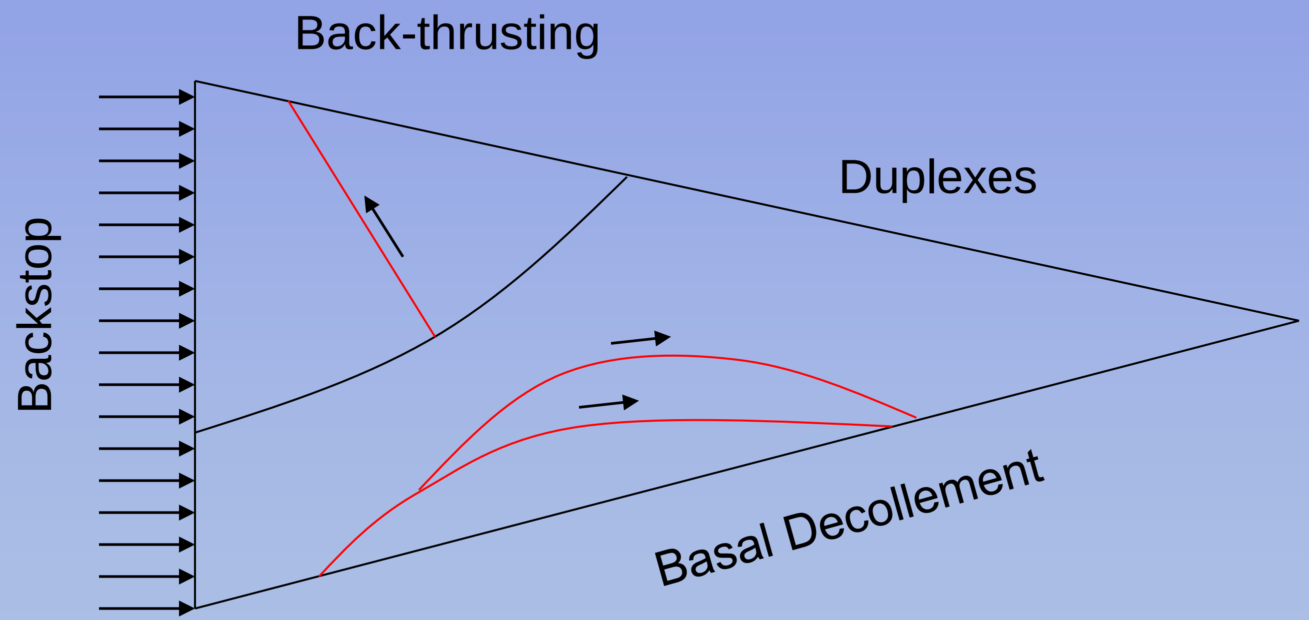

Effect of Erosion

Wedges that are forced into a persistant subcritical state by removal of material from their upper surface may undergo an extended period of internal deformation (e.g., DeCelles and Mitra, 1995). Continued formation of new duplex structures can lead to relatively high rates of material exhumation from the interior of the wedge (e.g., Konstantinovskaia and Malaveille, 2005).

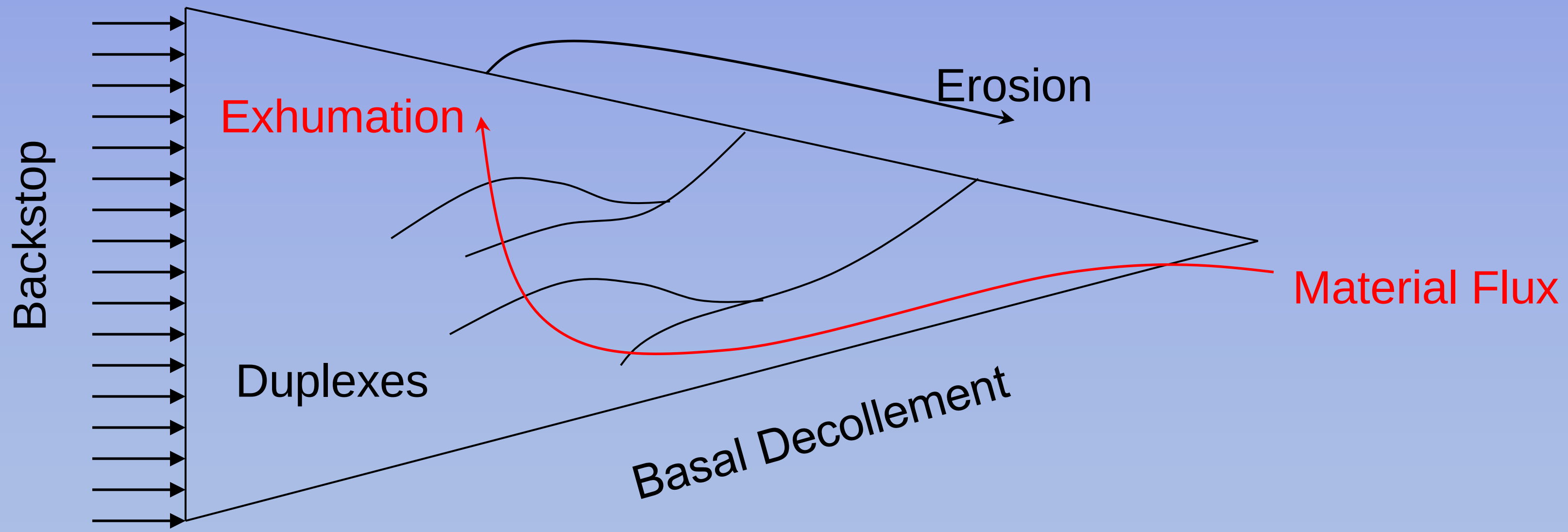

THE HIMALAYAN WEDGE

(Mukul, 2010)

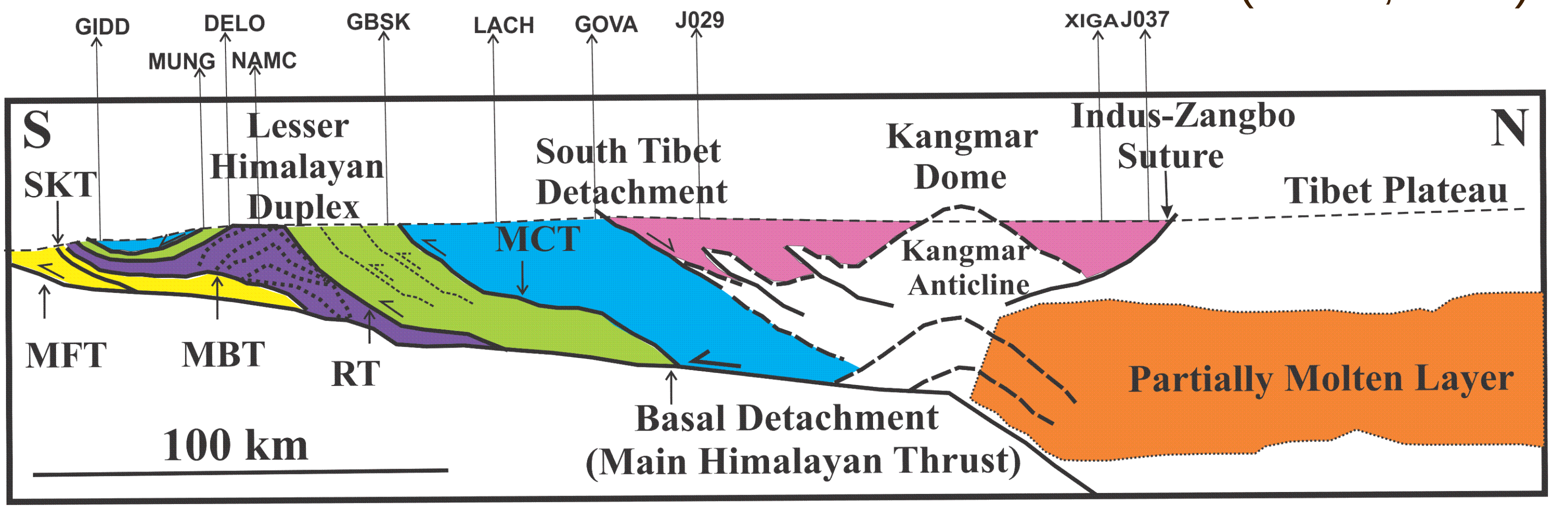

HIMALAYAN WEDGE

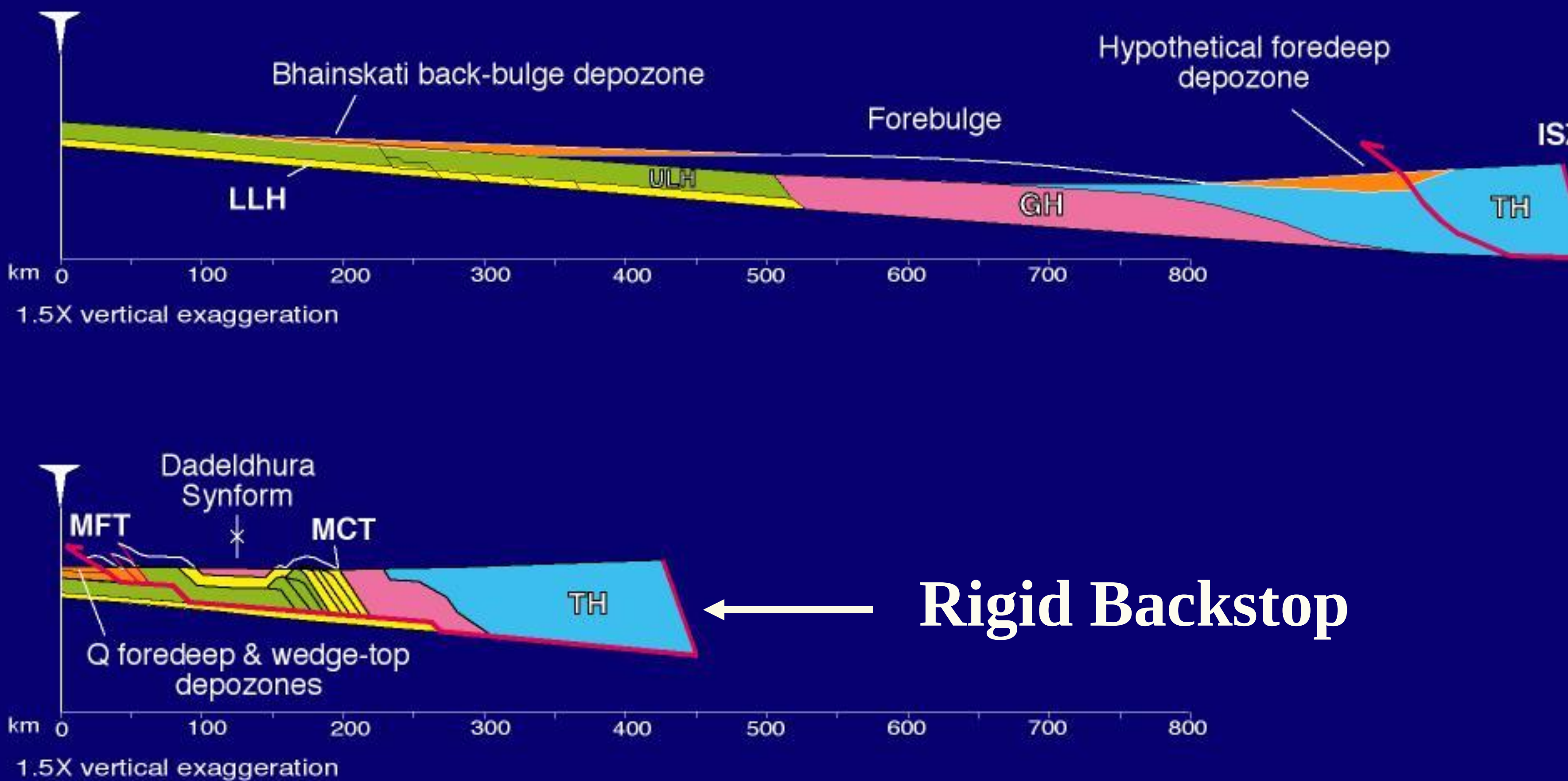

Rigid Backstop

Pete DeCelles – Nepal Hima

Pliocene to present (~3-0 Ma):
1. Emplacement of MFT sheets
2. Continued folding of Dadeldhura synform and passive uplift and tilting in hinterland (MCT and STDS)

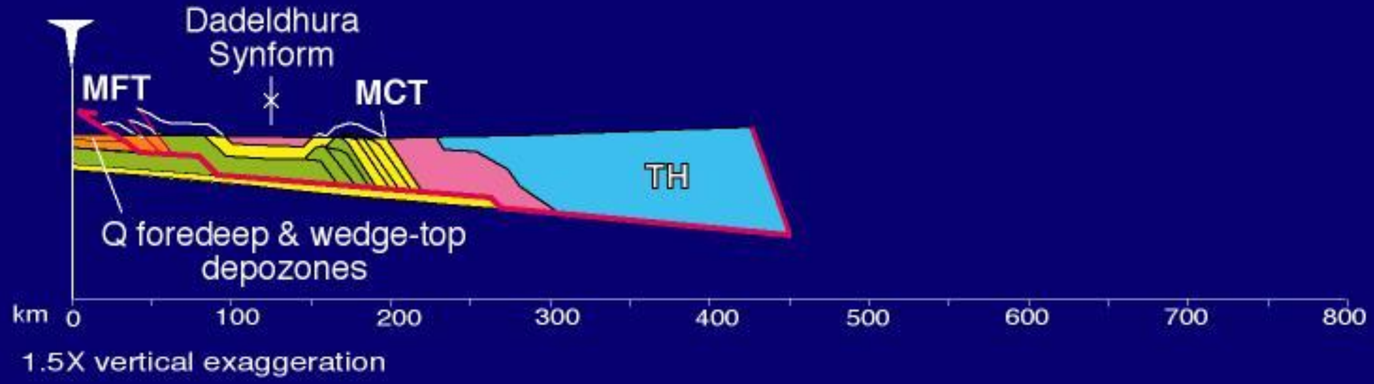

Mid—Late Miocene (~12-10 Ma):
1. Initial duplexing in LHZ
2. Passive tilting of MCT and STDS

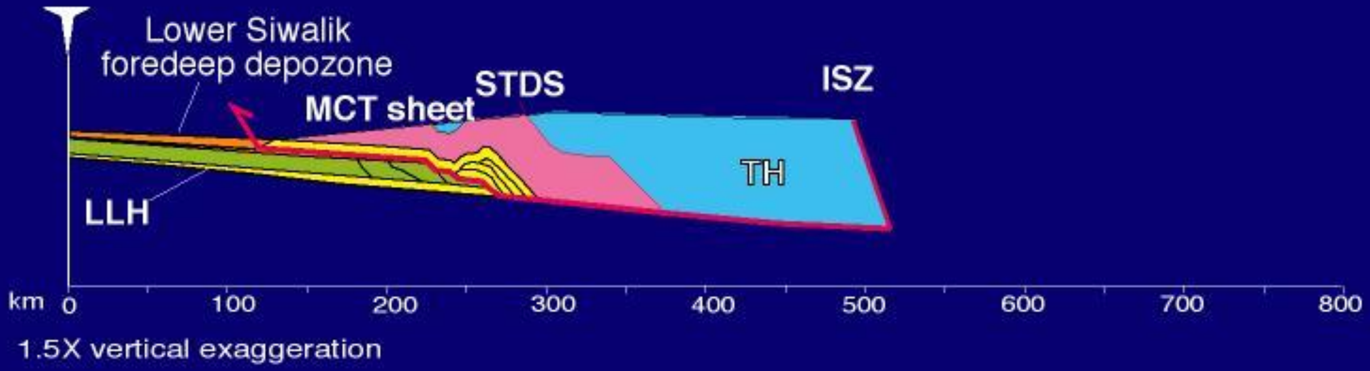

Early—Mid Miocene (~15-12 Ma):
1. Emplacement of Ramgarh thrust sheet
2. Deposition of lower Siwalik foredeep

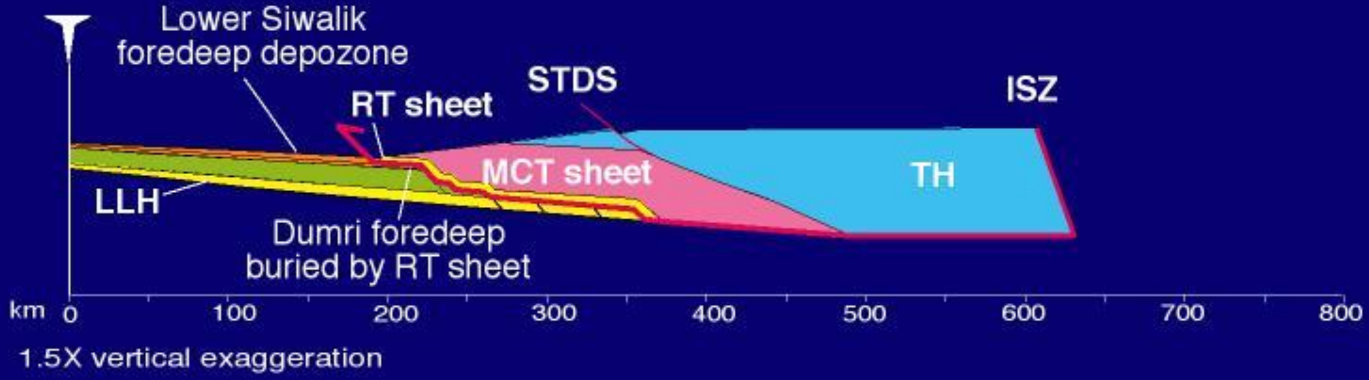

Eocene:
1.Development of Tethyan thrust belt
2. Metamorphism of GH rocks

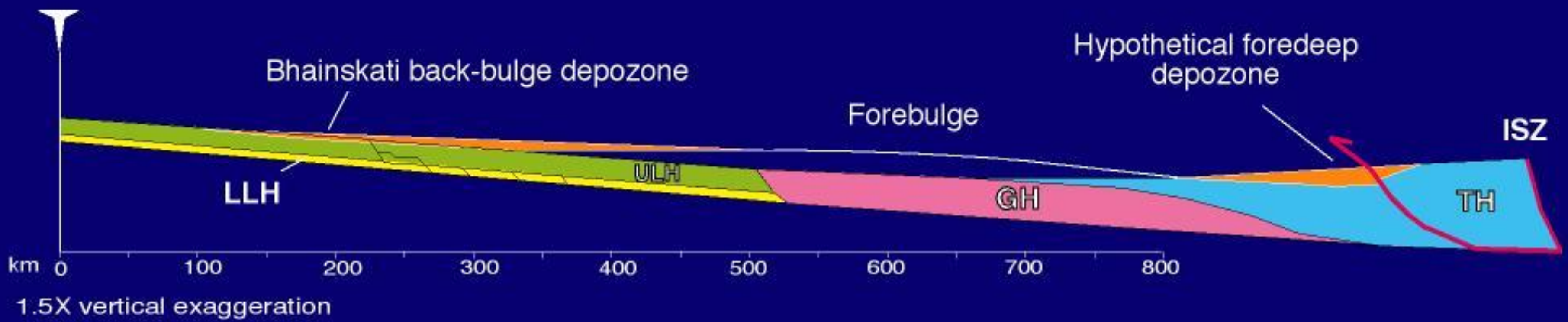

SHORTENING

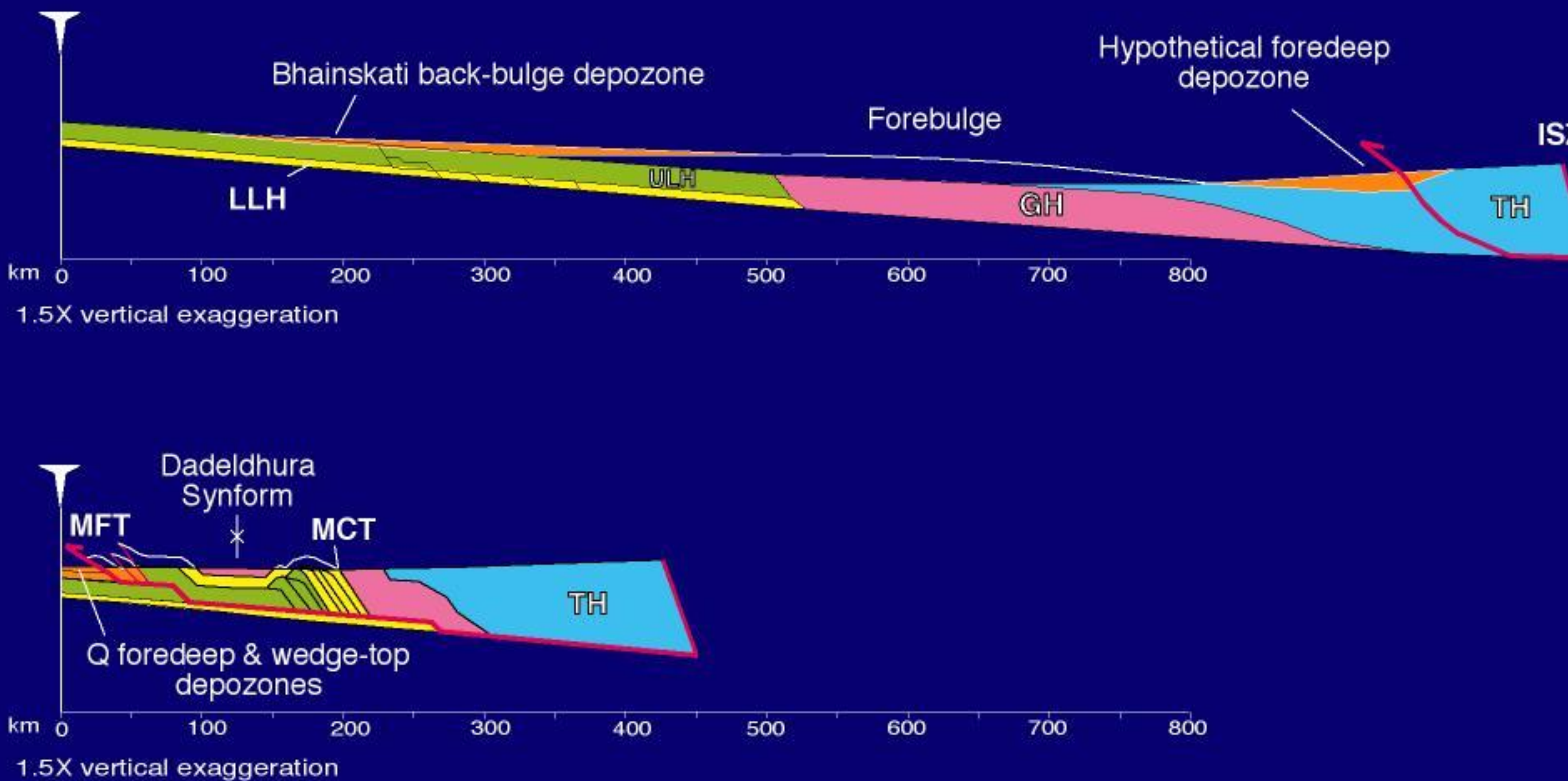

Pete DeCelles – Nepal Himalaya

The Himalaya as a Critically Tapered Orogenic Wedge

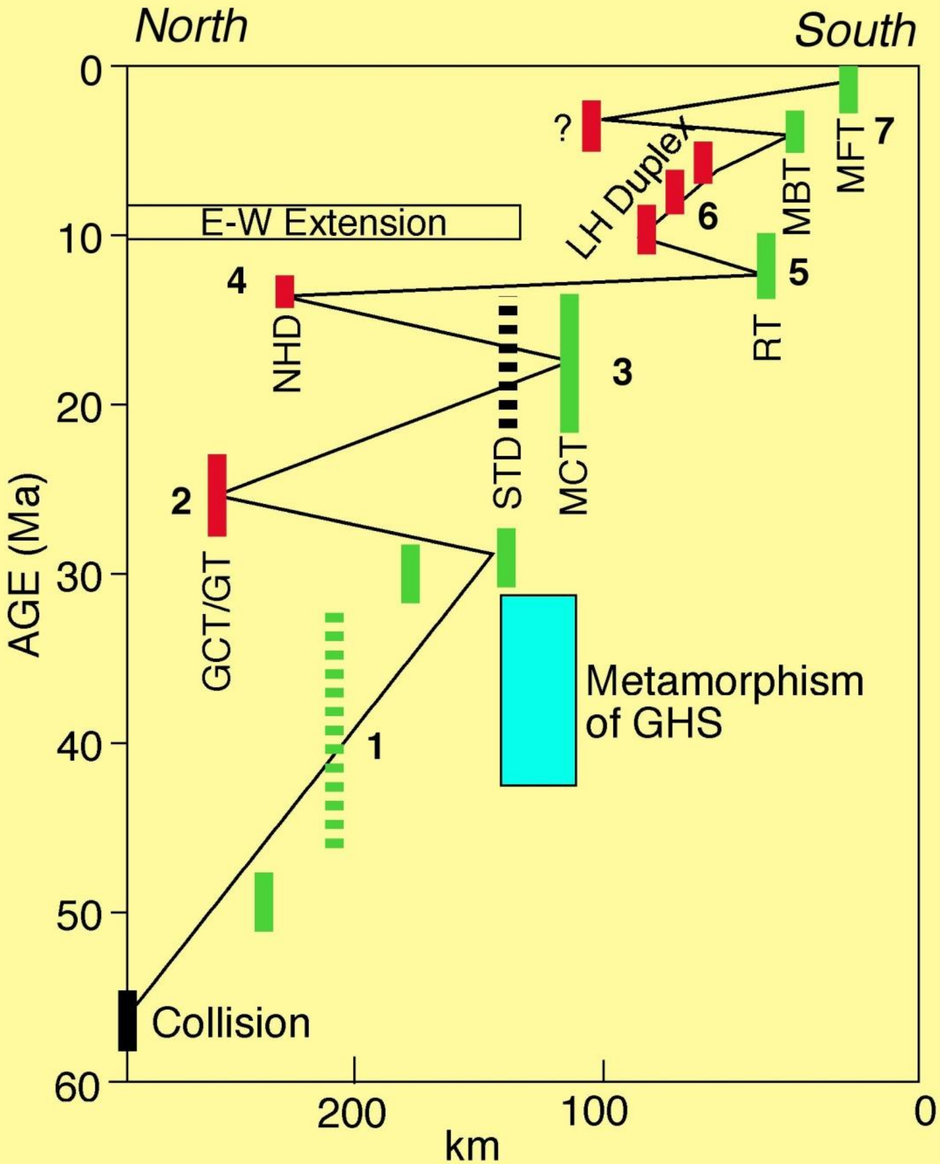

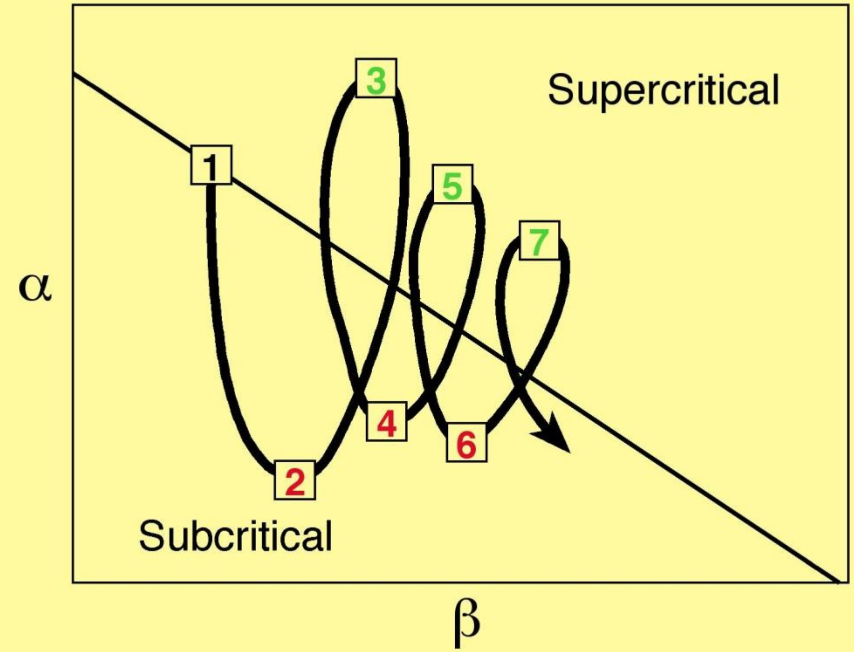

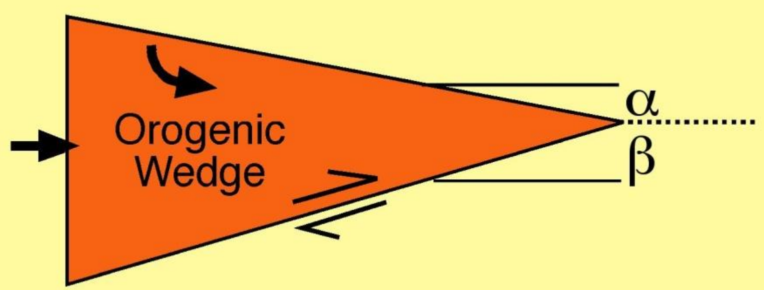

Mukul et al (Geology, Nov. 2007)

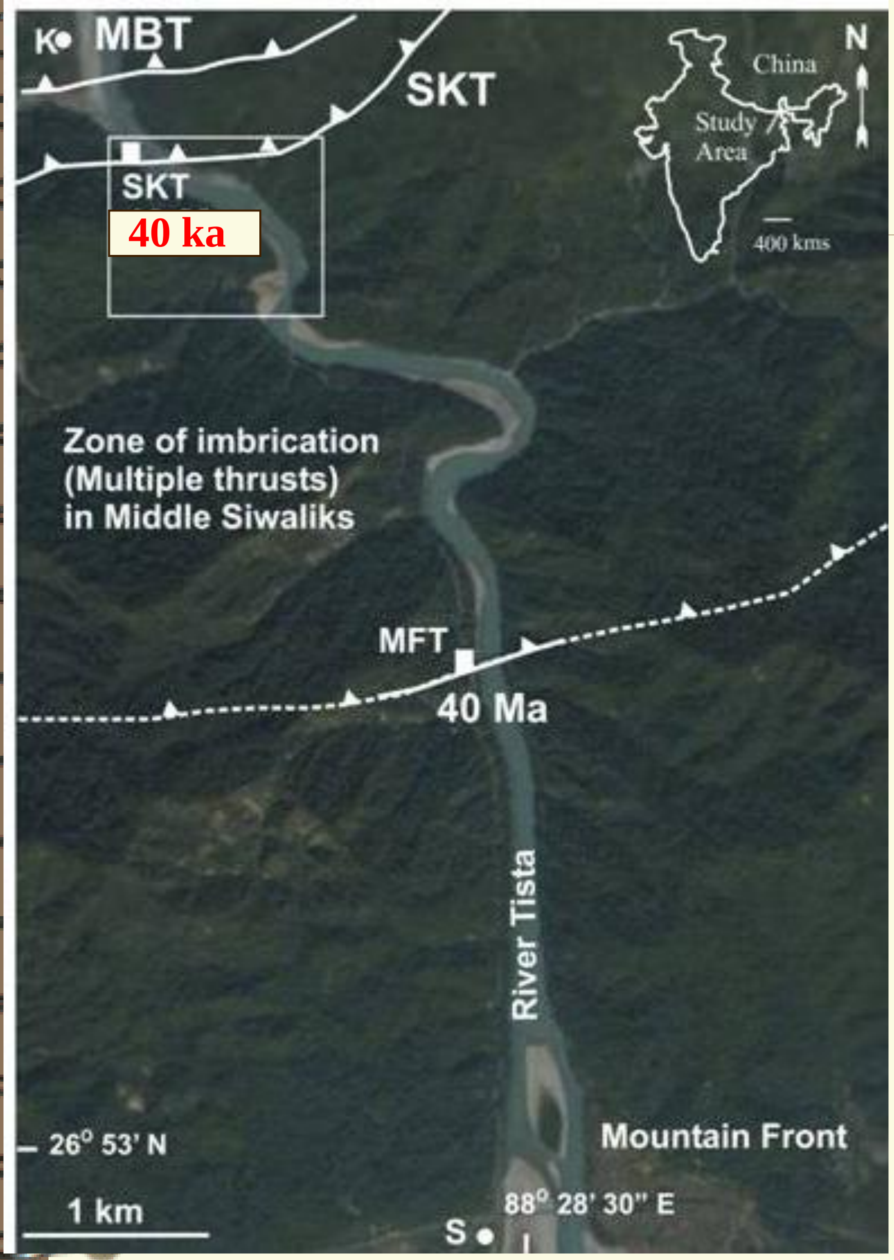

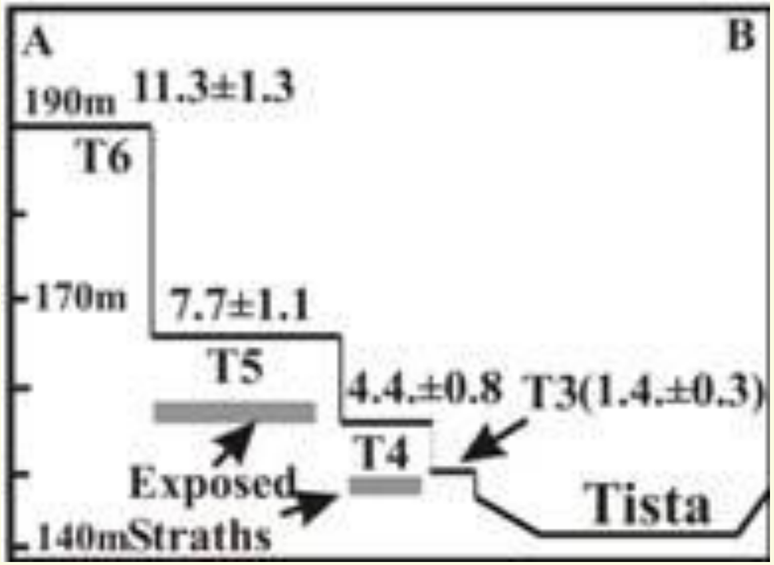

THE HIMALAYAN WEDGE

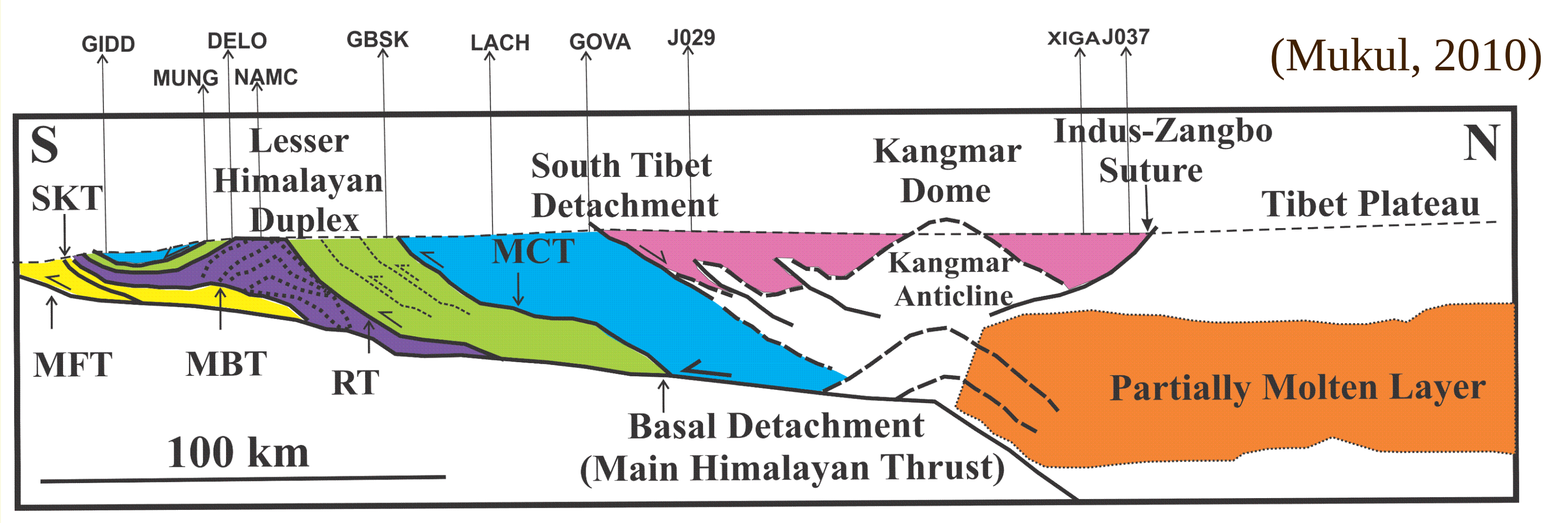

Basal Décollement Main Himalayan Thrust

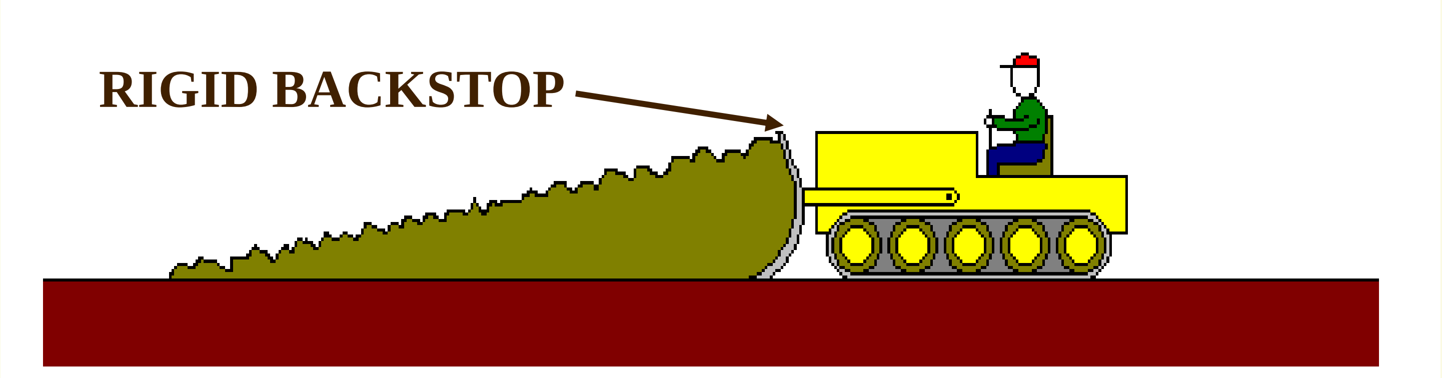

RIGID BACKSTOP

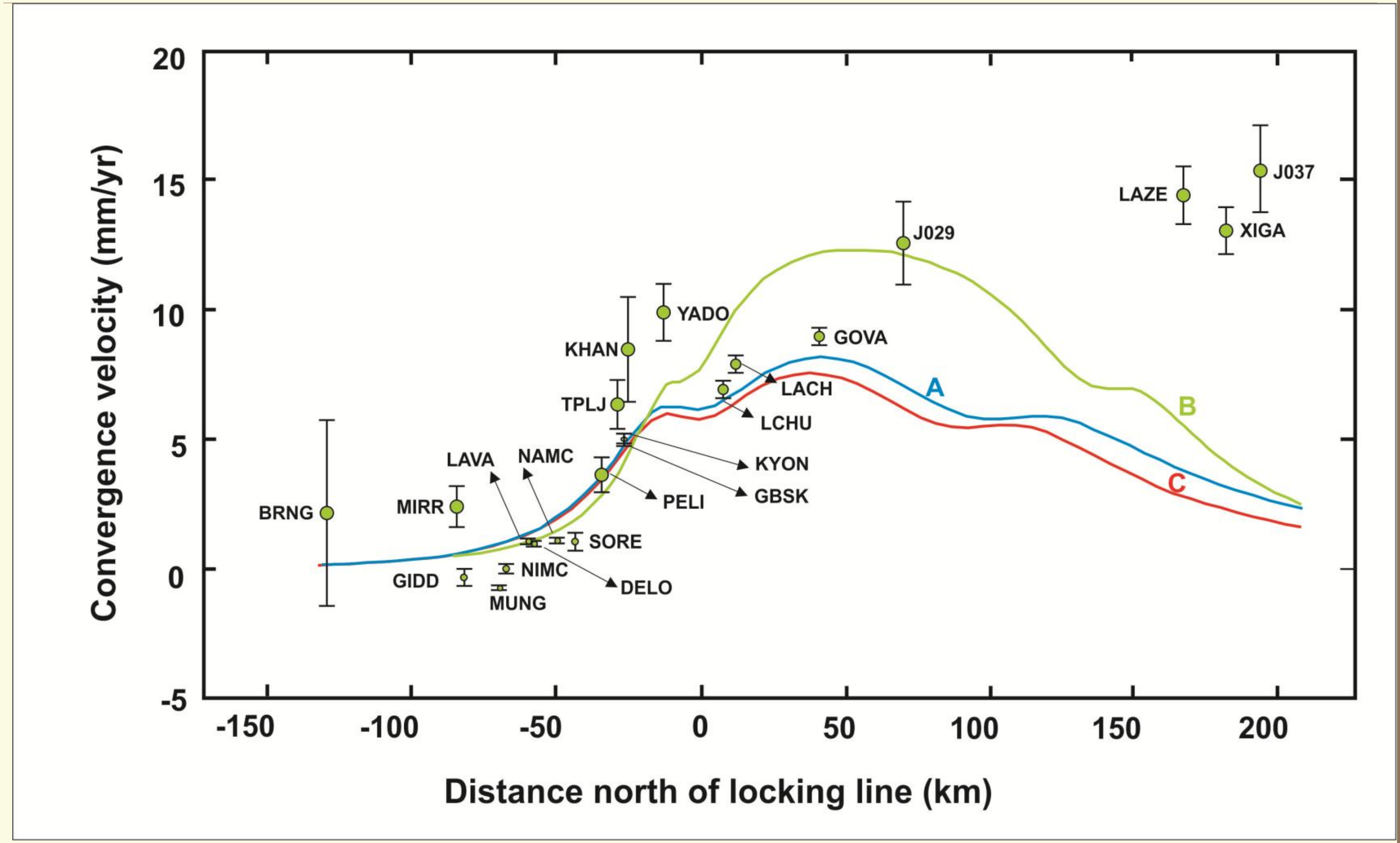

THE HIMALAYAN WEDGE

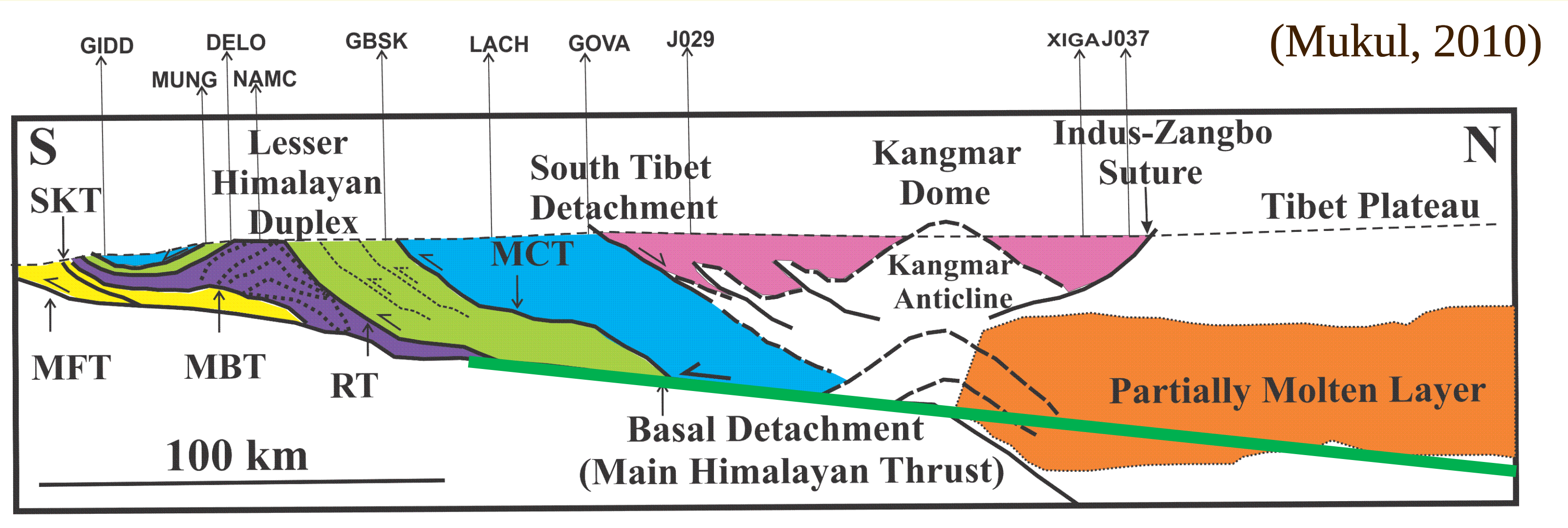

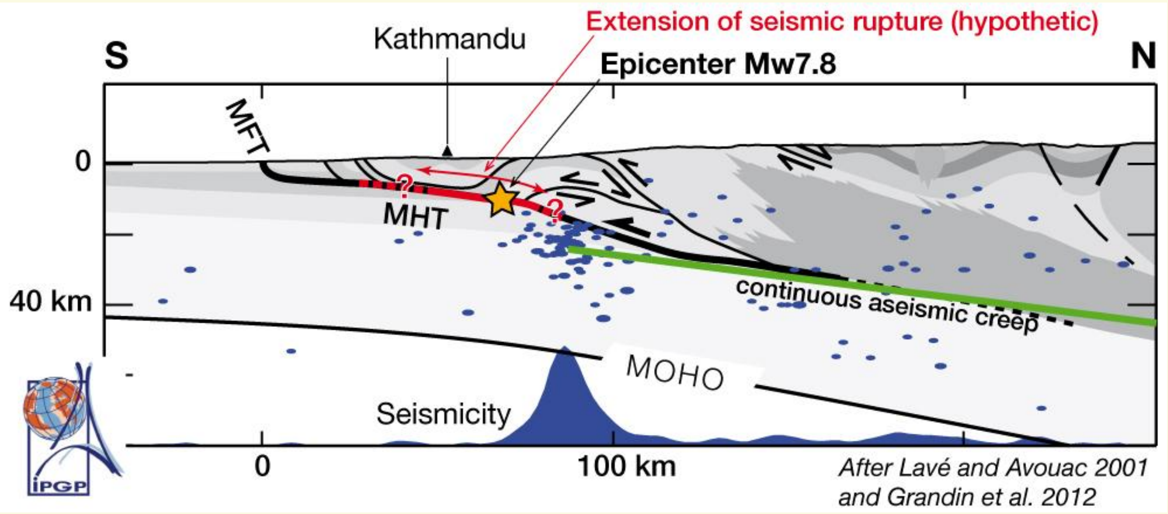

Elastico-Frictional Wedge underestimates hinterland velocities

DEFORMABLE BACKSTOP

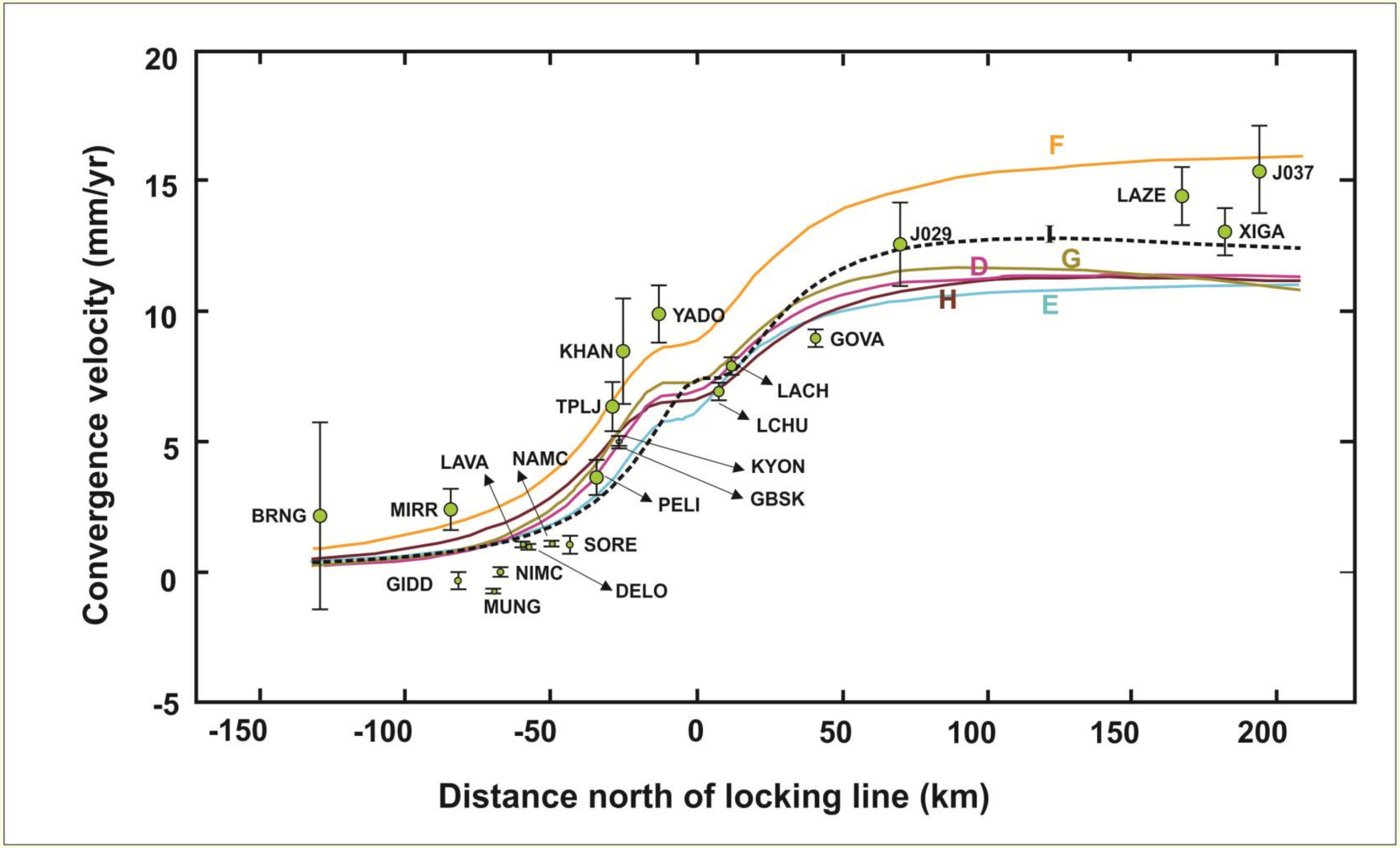

(Stevens and Avouac, 2015)

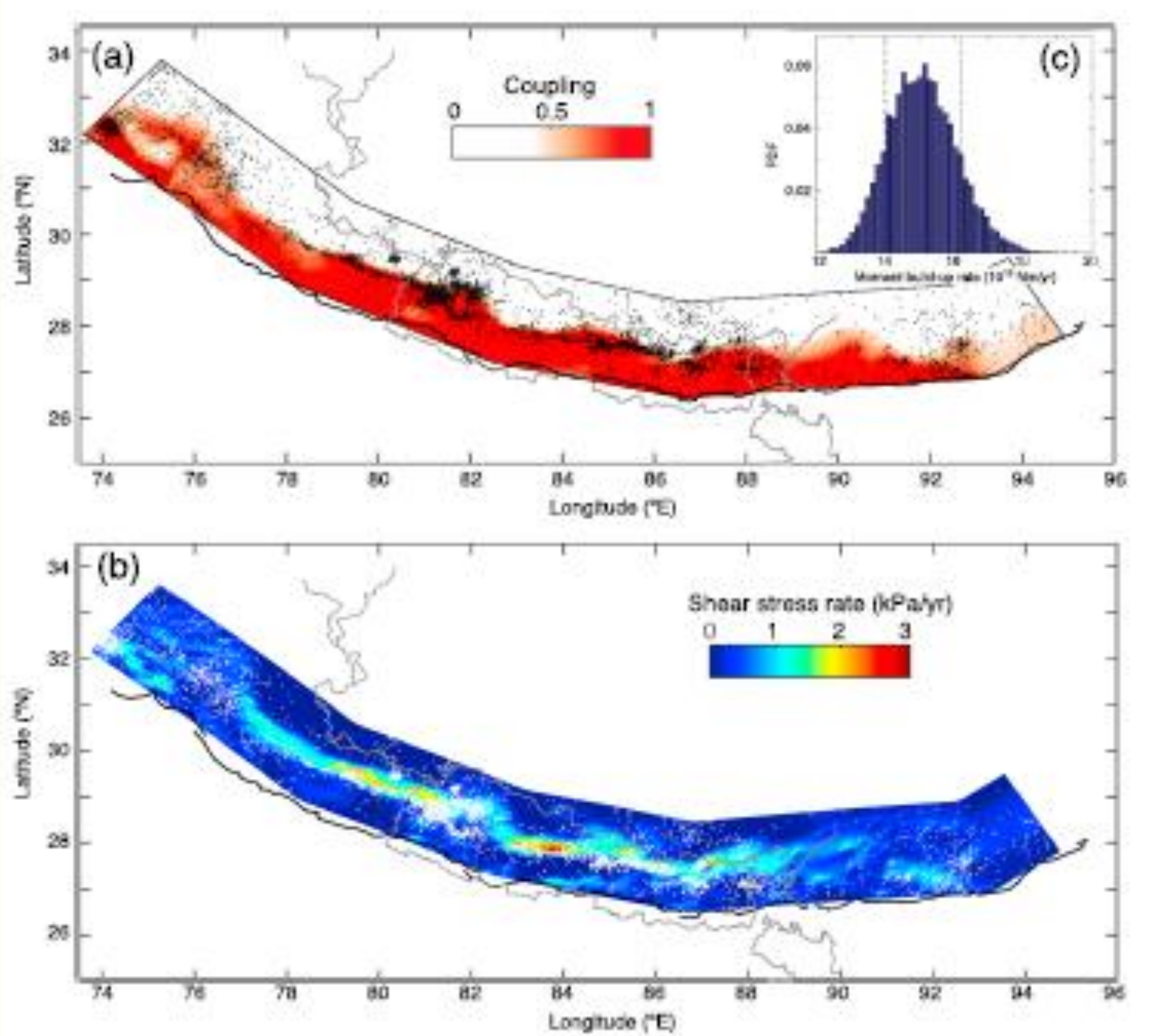

HIMALAYAN ARC

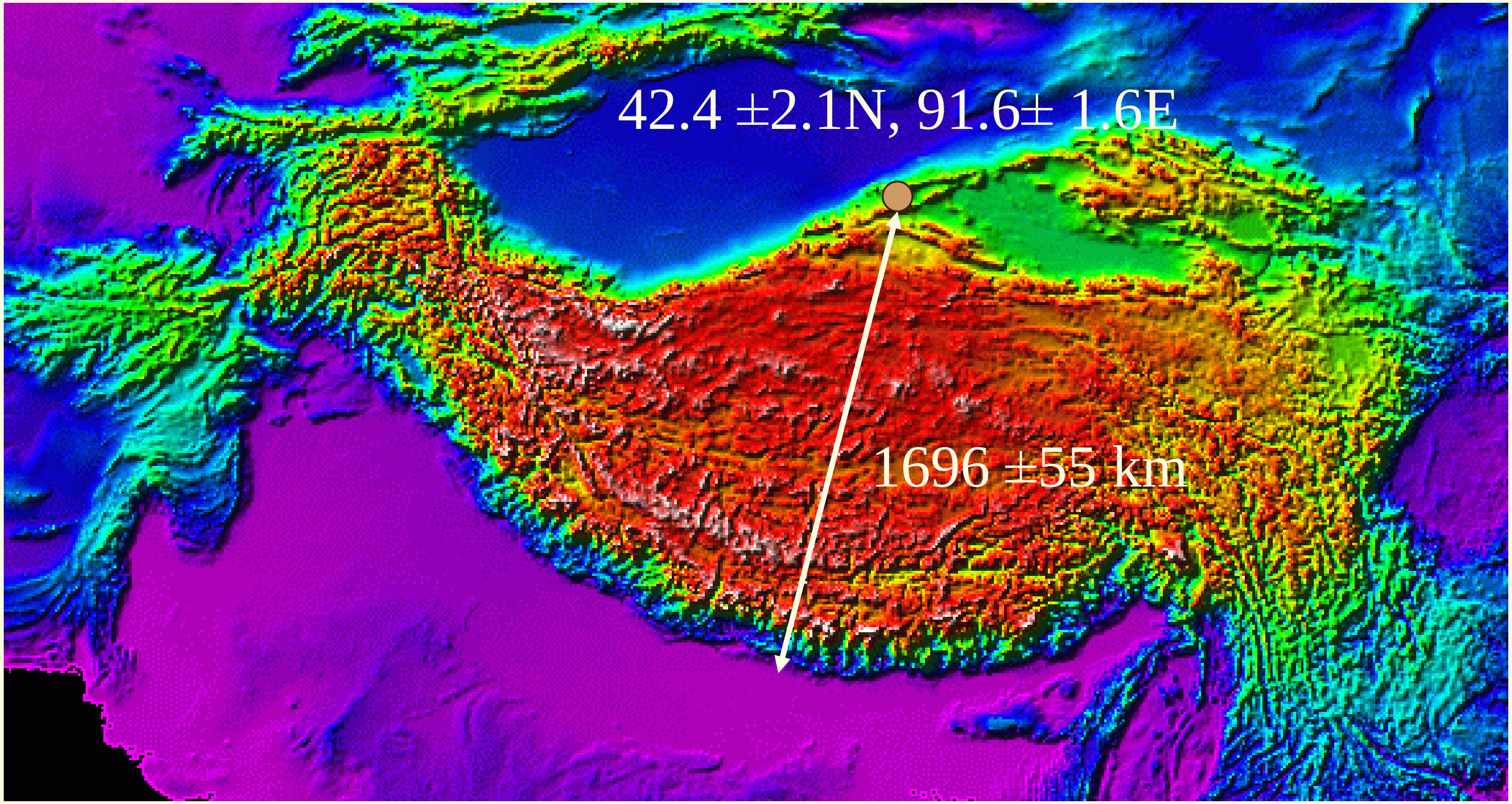

http://www.geo.cornell.edu/grads/duncan/topo/topo.gif

(Bendick and Bilham, Geology, 2001)

MAKING OF THE ARC

- Mountain belts have a wedge shaped geometry since they develop from a wedge shaped sedimentary prism with taper given by sum of basal slope (β) & surface slope (α)
- Kinematics - elastico-plastic deformation with deformable backstop
- Responsible For EARTHQUAKES

BREAKING THE ARC

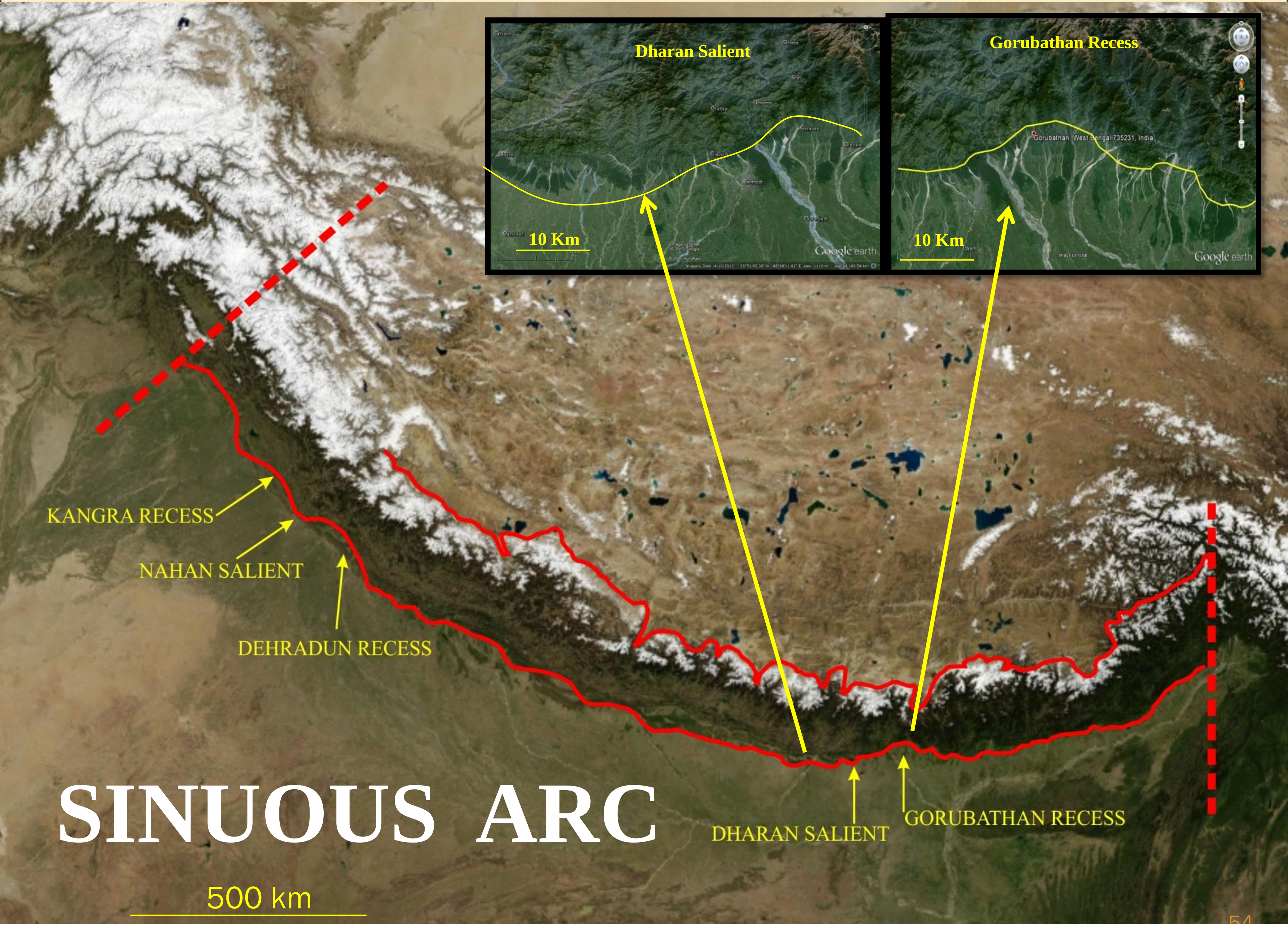

https://upload.wikimedia.org/wikipedia/en/2/25/Himalayas_landsat_7.png

EASTERN HIMALAYA

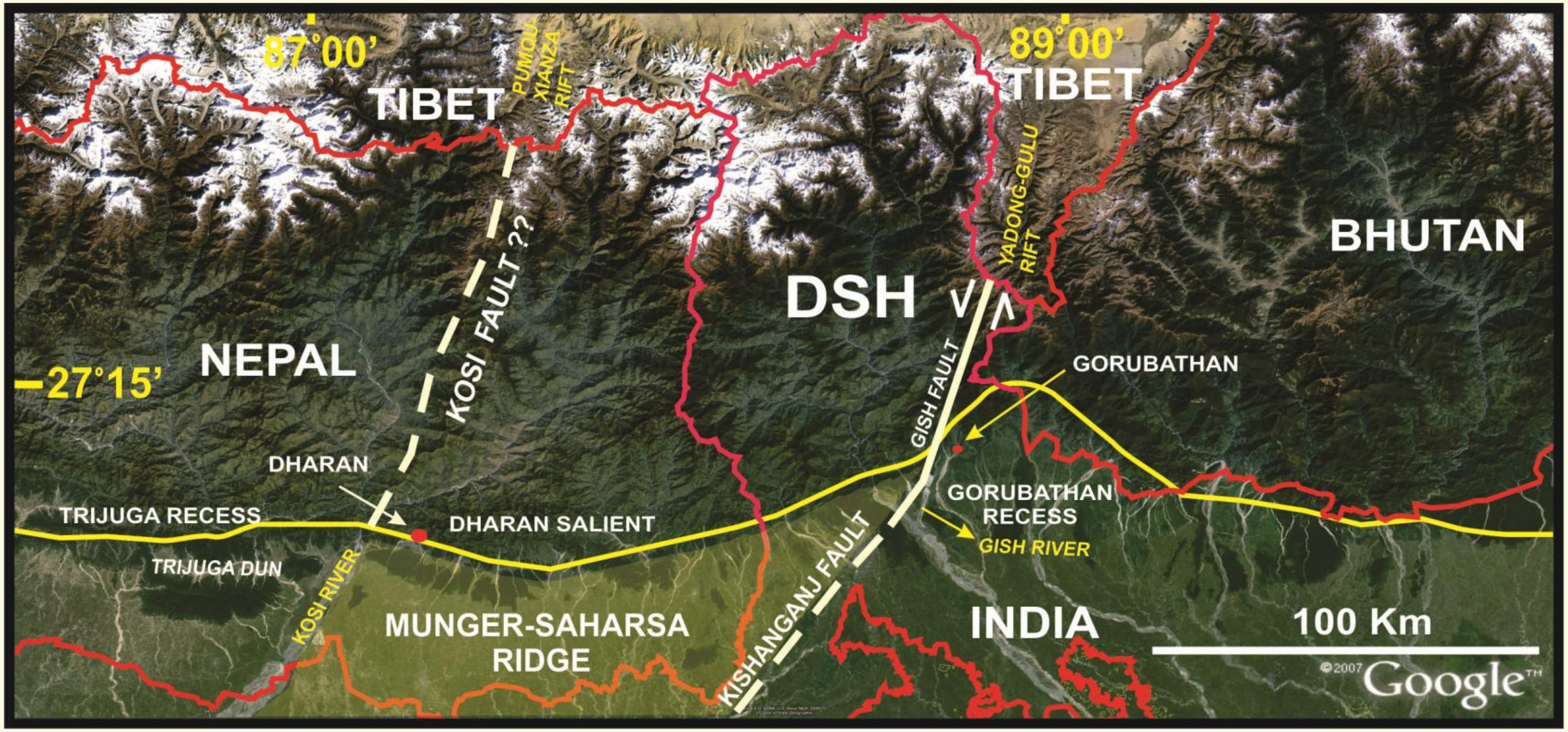

FRONTAL STRUCTURE

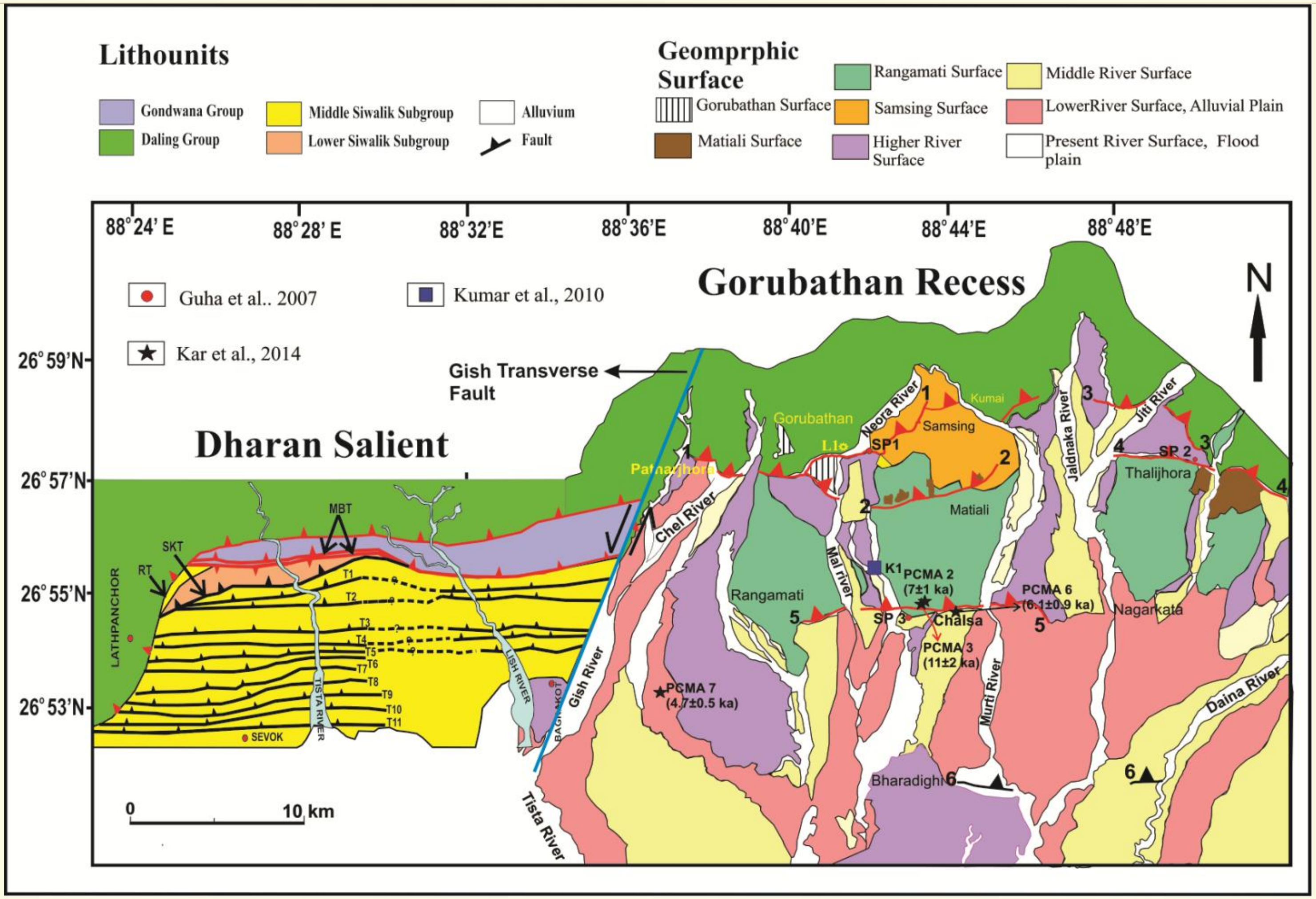

Srivastava and Mukul, (2015)

(Mitra et al, 2010)

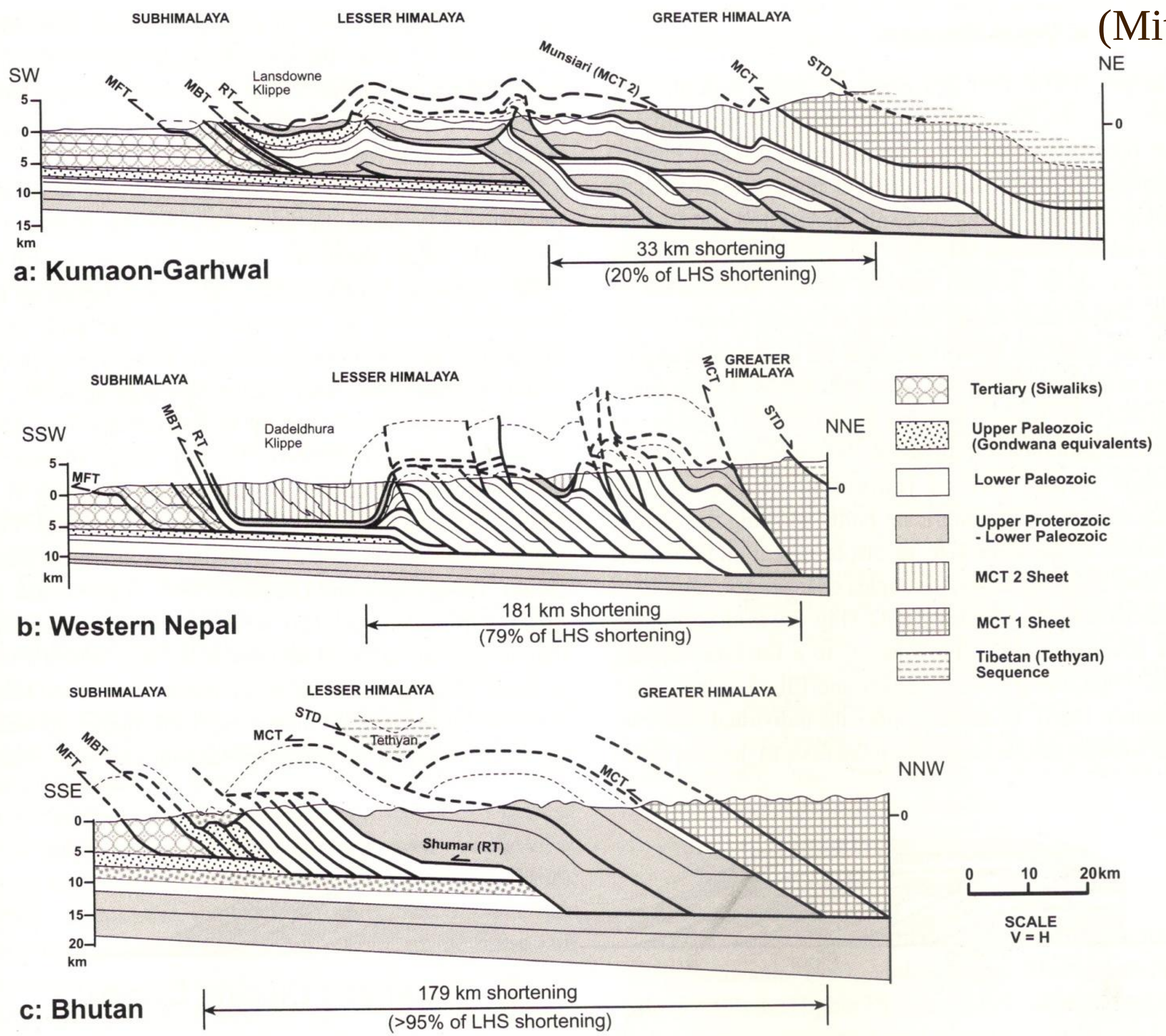

Fig.2. Regional balanced cross-sections through the Himalayas in **(a)** Kumaon (*after* Srivastava and Mitra, 1994), **(b)** western Nepal (*after* DeCelles et al. 1998) and **(c)** Bhutan (after McQuarrie et al., 2008) showing the principal tectonic features and the variation in geometry and stratigraphic position of the Lesser Himalayan Duplex that carries crystalline complexes along its roof thrust. See Fig.1 for locations of cross-sections.

(Mitra et al, 2010)

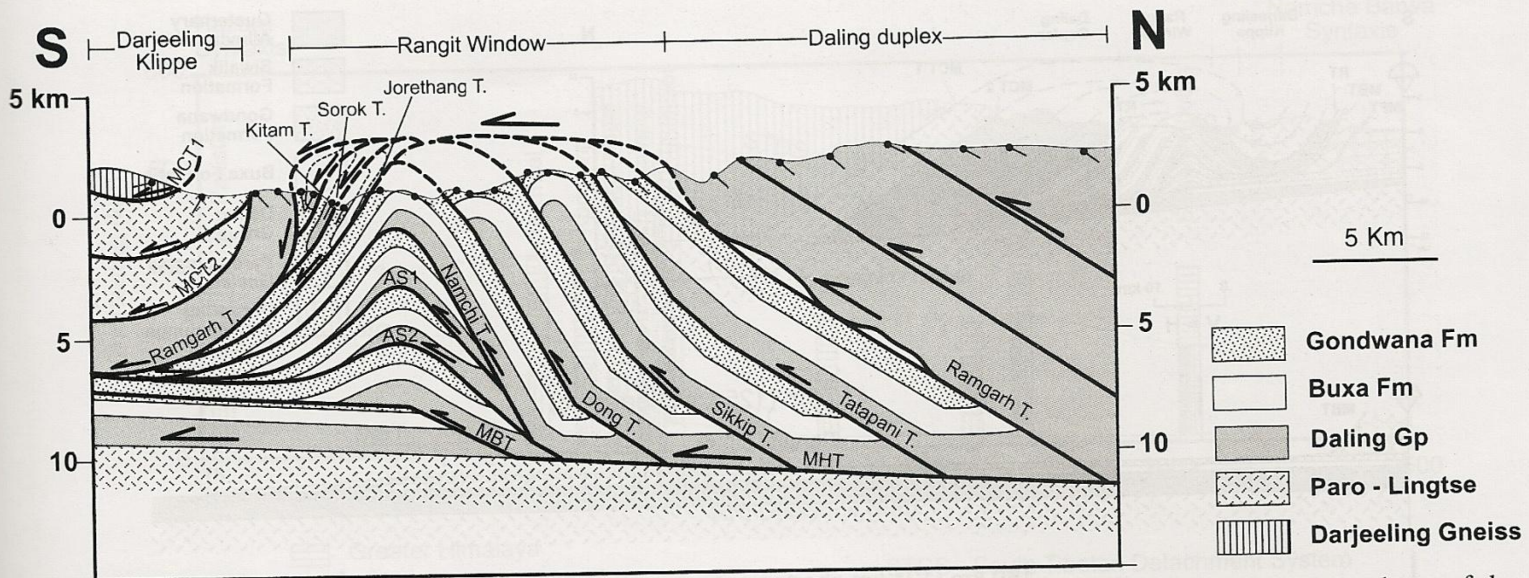

Fig.6. Balanced N-S cross-section through the Rangit duplex showing the northern hinterland dipping component made up of three horses, the middle antiformal stack with three horses, and the southern foreland dipping component made up of three horses. The roof thrust is the folded Ramgarh thrust carrying the Daling duplex in its hanging wall at the north end of the section. The floor thrust is the Main Himalayan sole thrust (MHT).

2015 NEPAL GURKHA EARTHQUAKE

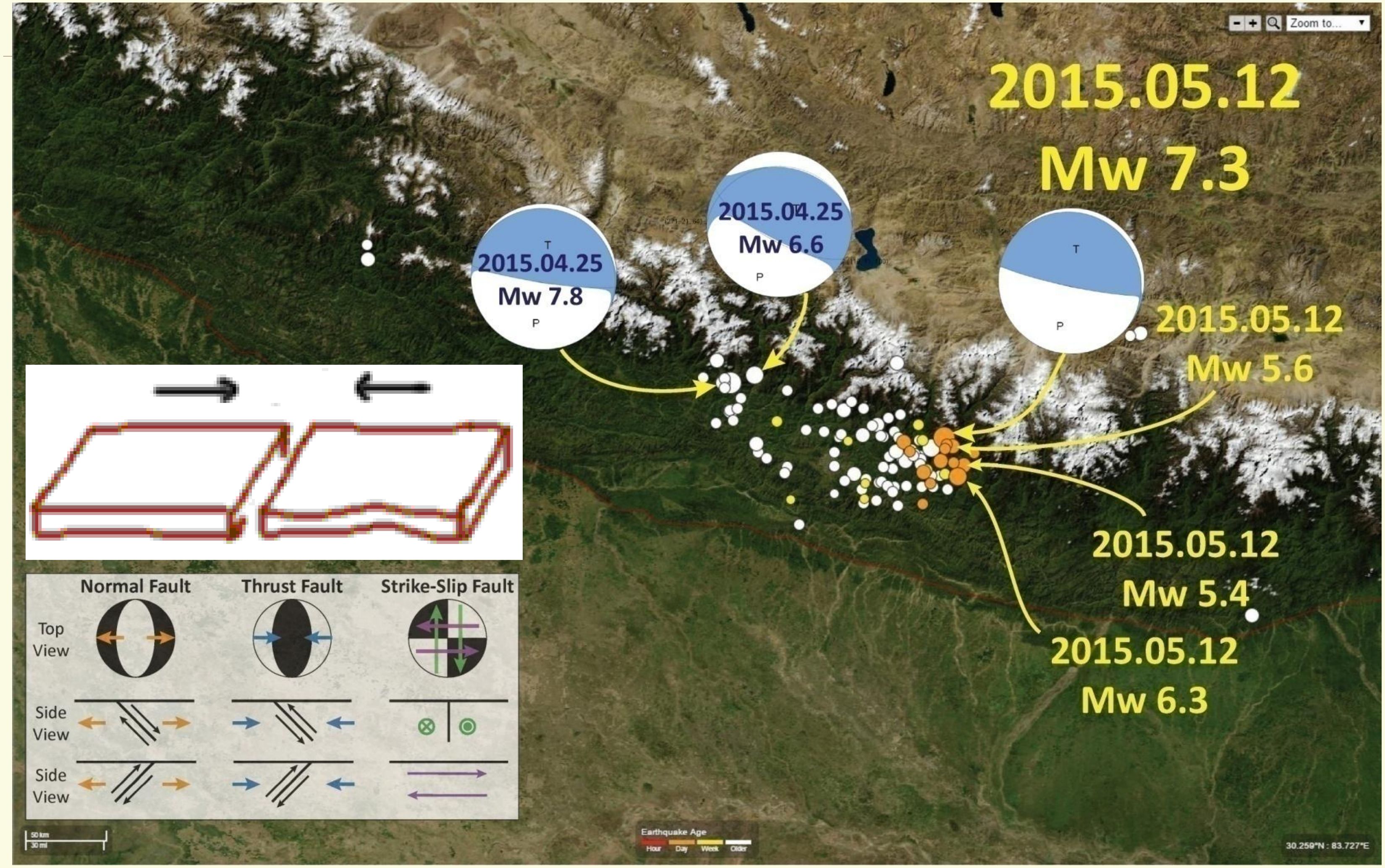

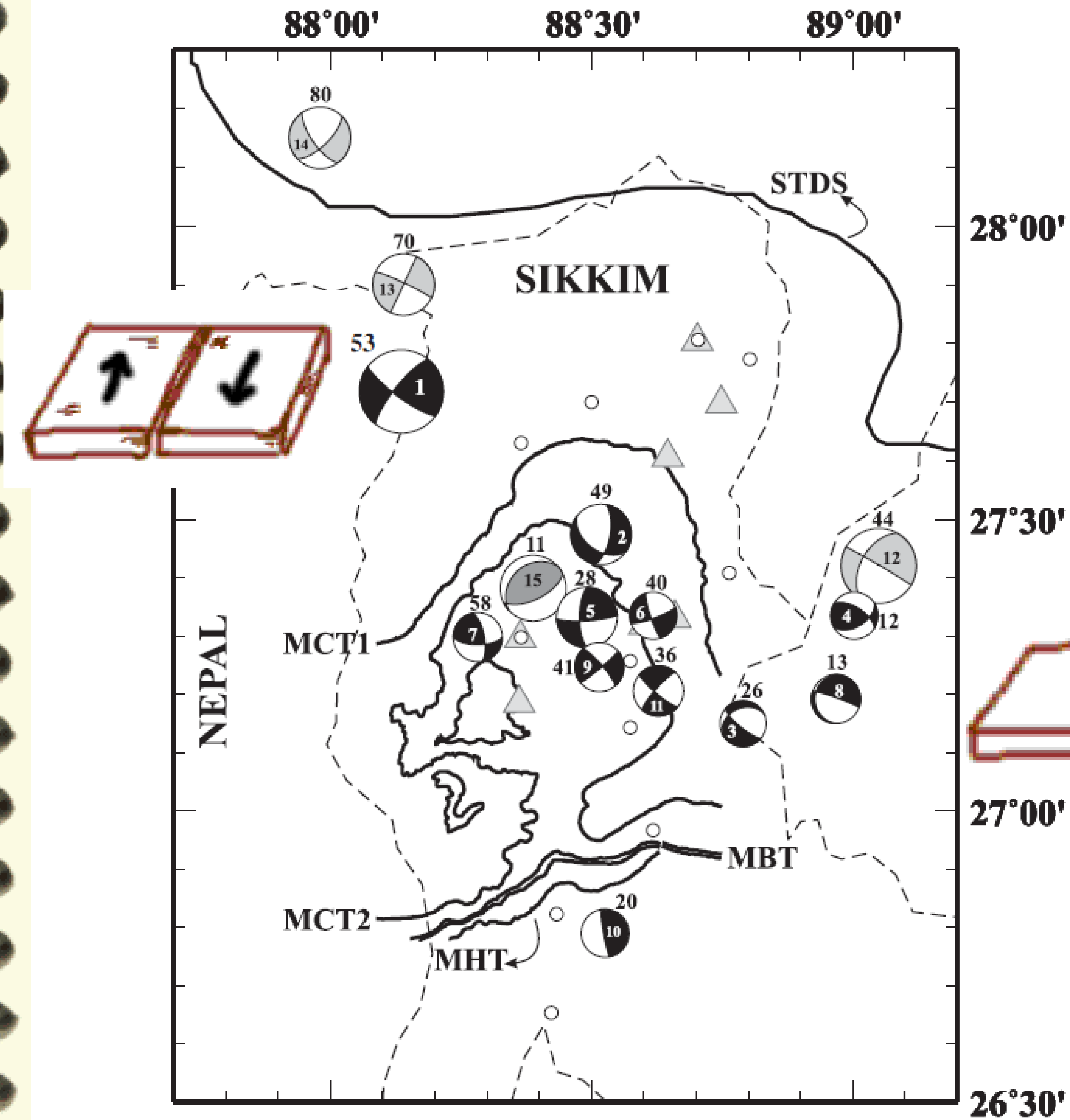

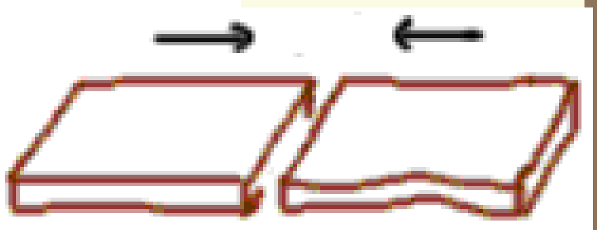

Paul et al (2015, GJI)

EARTHQUAKE IN SIKKIM ON SEP 18, 2011

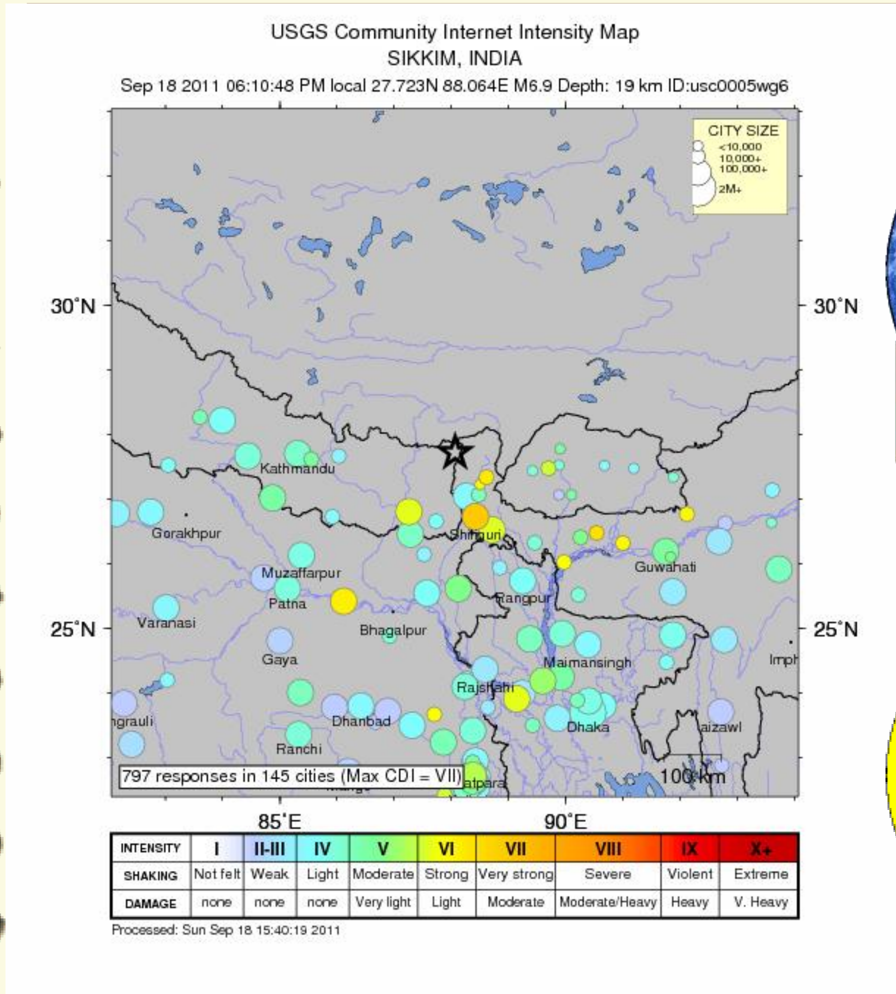

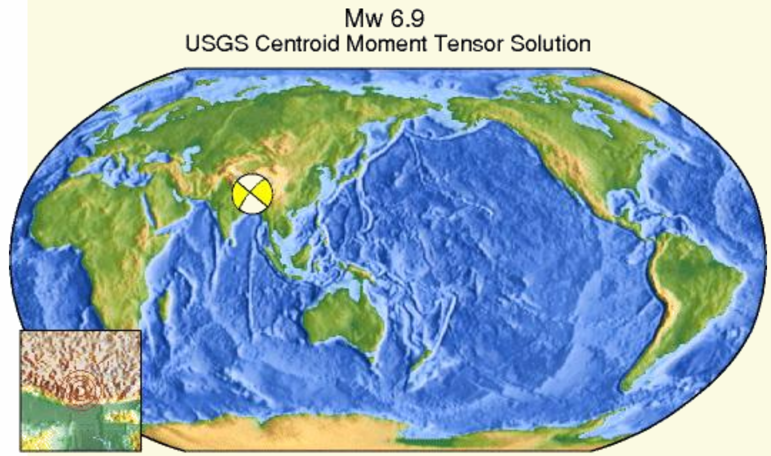

Date: 18 SEP 2011
Time: 12:40:51.55
Epicenter: 27.740 88.113
Depth: 35 km

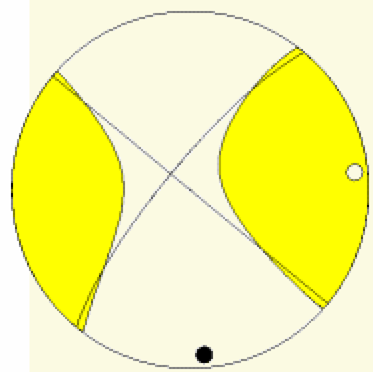

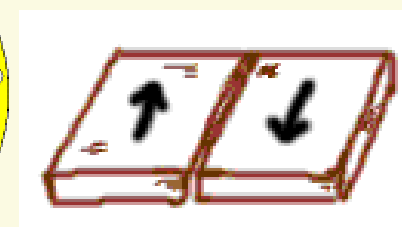

DARJEELING-SIKKIM SEISMICITY

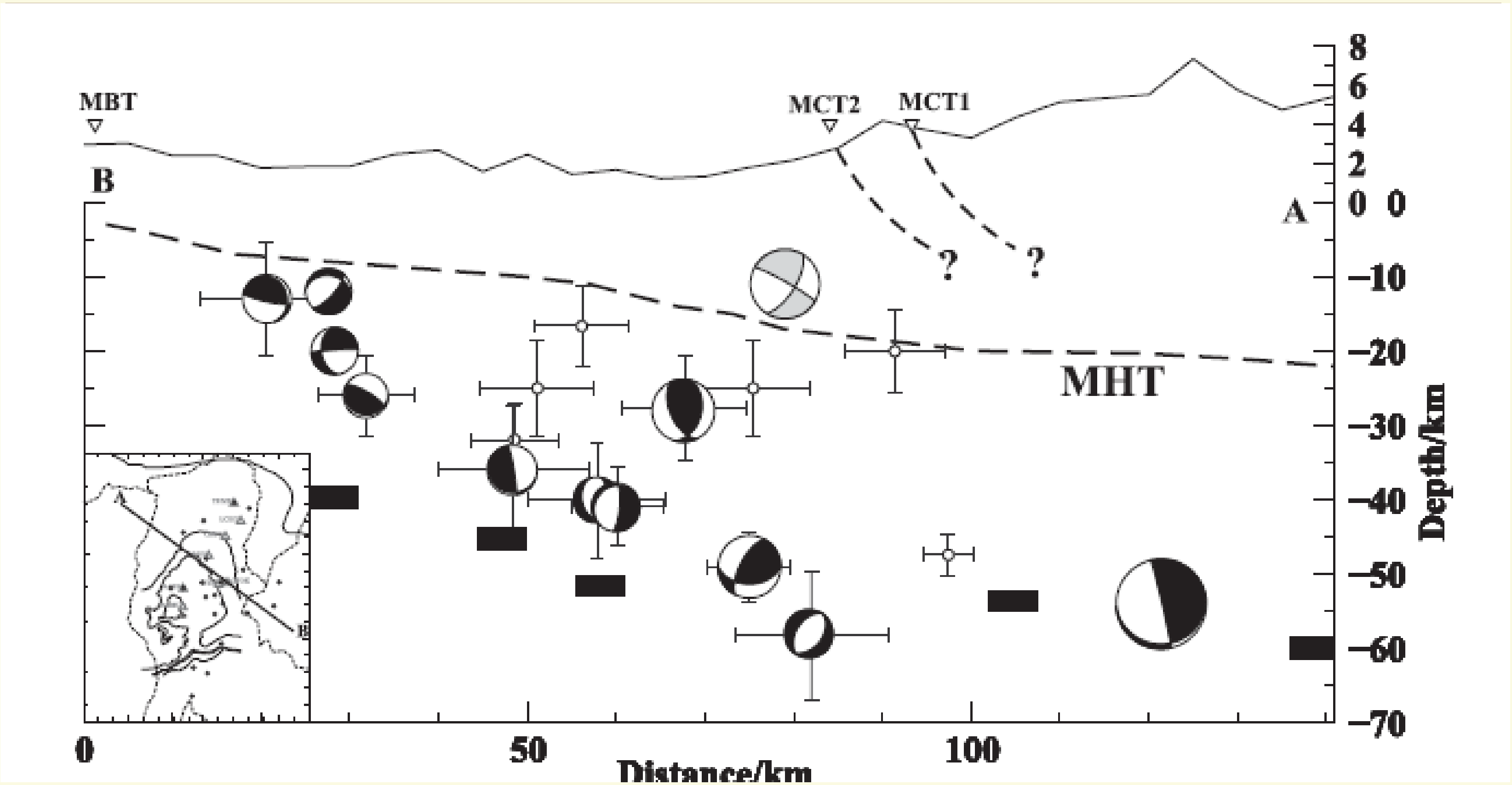

Paul et al (2015, GJI)

Broken Himalayan Arc

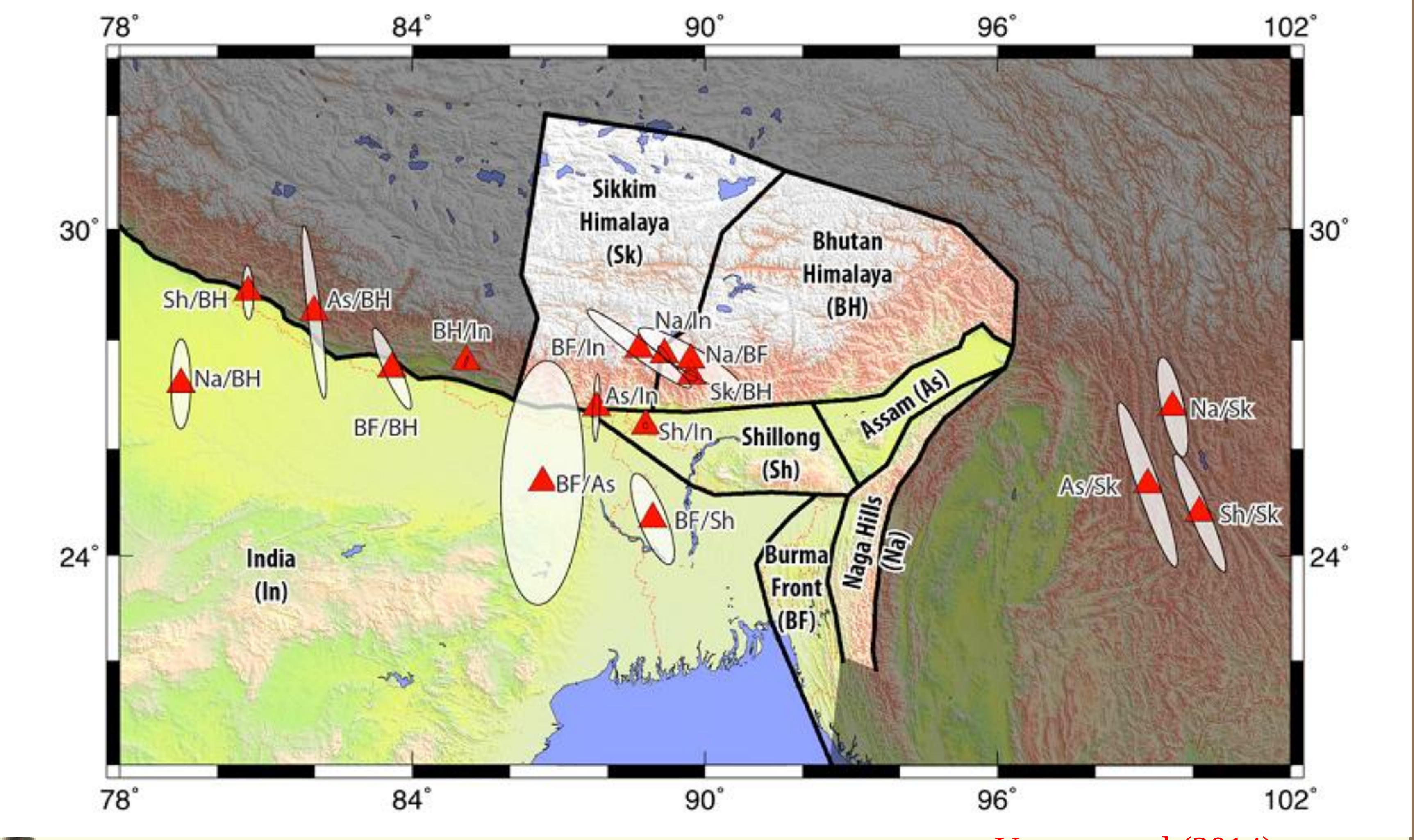

Vernant et al (2014)

BREAKING OF THE ARC

- How many segments in the arc?
- Will decollement-earthquake ruptures remain confined to one segment?
- Overall Implications of segmentation on Earthquake hazard in the Himalaya

ACKNOWLEDGMENTS

- Talk is the result of work and discussions many colleagues and students:

  Prof. V. K. Gaur, Sridevi Jade, Abdul Matin,
  Prof. K.S. Valdiya, Pete Decelles,
  Roger Bilham, Gautam Mitra

- Research Funded by DST, NSF-USA, IITB


Thank You!
For your attention!